CHALMERS

Analysis of reinforced concrete slabs strengthened with textile reinforcement

Non-linear Finite Element Analysis

Master of Science Thesis in the Master's Programme Structural Engineering and Building Performance Design

DRAGOS PETRE
IWONA ZAPALOWICZ

Department of Civil and Environmental Engineering
Division of Structural Engineering
Concrete Structures
CHALMERS UNIVERSITY OF TECHNOLOGY
Göteborg, Sweden 2012
Master's Thesis 2012:87

Analysis of reinforced concrete slabs strengthened with textile reinforcement

Non-linear Finite Element Analysis

Master of Science Thesis in the Master's Programme

DRAGOS PETRE

IWONA ZAPALOWICZ

Department of Civil and Environmental Engineering
Division of Structural Engineering
Concrete Structures

CHALMERS UNIVERSITY OF TECHNOLOGY
Göteborg, Sweden 2012

Cover:
Figure: Finite Element Analysis of bending slab at failure.

Analysis of reinforced concrete slabs strengthened with textile reinforcement
Non-linear finite element analysis
Master of Science Thesis in the Master's Programme
DRAGOS PETRE
IWONA ZAPALOWICZ
Department of Civil and Environmental Engineering
Division of Division of *Structural Engineering*
Concrete Structures
Chalmers University of Technology

ABSTRACT

Reinforced Concrete (RC) has become one of the most commonly used materials up to now. Despite their efficiency, RC structures have posed some disadvantages, primarily related to durability and corrosion of steel reinforcement. Just over a decade ago, however, a new concept has been developed with the idea of replacing the steel reinforcement with alkali-resistant textile fibres resulting in a new composite material called Textile Reinforced Concrete (TRC). This new construction material offers important advantages such as resistance to corrosion and thinner and lighter structures. An application which has become of great interest as of late is the use of TRC in rehabilitation, such that it can strengthen different structural elements like slabs, beams or columns.

The main purpose of this report is to model and analyse the effects of strengthening RC structures using TRC layers, particularly focusing on a TRC strengthened RC slab. The main method used in this project was numerical modelling based on the Finite Element Method (FEM). The finite element software DIANA FX+ was utilized to develop a 2-D non-linear model of a TRC strengthened RC slab. The verification of the developed model was accomplished by means of experimental and numerical results from a previous study.

The results showed that the RC slabs strengthened with TRC present significant increase in the load-bearing capacity compared to the unstrengthened RC slabs. Furthermore, for a similar load level, the final deflection was reduced in the case of strengthened slabs. The hand calculations of the ultimate load were consistent with the numerical results.

This project has shown the efficiency of strengthening RC slabs with TRC layers. The modelling of the bond-slip relation between concrete and reinforcement using interface elements lead to a parametric study of this behaviour. This showed the importance of implementing interface elements instead of embedded reinforcement with full interaction in order to achieve realistic results. Further analysis of bi-directional slabs using 3D modelling is recommended for a better representation of the bonding behaviour between the textile reinforcement and the concrete.

Key words: Non-linear finite element analysis, textile reinforced concrete, slabs, interface elements, bond-slip behaviour

Contents

Preface

In this study, numerical modelling using Finite Elements Method was effectuated. The work in this thesis was carried out from January 2012 to June 2012 at the Department of Civil and Environmental Engineering, Division of Structural Engineering, Concrete Structures, Chalmers University of Technology.

It was a pleasure to do research at Chalmers under the supervision of M. Sc. Natalie Williams Portal and Professor Karin Lundgren who also was the examiner. We would like to thank them for guiding us through the development of this research, for their engagement and support.

We would also like to thank M. Sc. David Fall and our office colleagues Eyrún Gestsdóttir and Tómas Guðmundsson for their help.

Göteborg, June 2012

Dragos Petre and Iwona Zapalowicz

Notations

Roman upper case letters

A_c	Cross-section area of concrete in compression
A_s	Cross-section area of bottom longitudinal steel reinforcement
A_t	Cross-section area of textile reinforcement
CP	Contact Perimeter
E	Young's modulus
F	Force
F_c	Concrete force
F_s	Steel force
F_t	Textile force
FE	Finite Element
G_f	Fracture energy in tension
$I_{concrete}$	Concrete's moment of inertia
I_{steel}	Steel's moment of inertia
$I_{textile}$	Textile's moment of inertia
K_{slab}	Rigidity of the slab
M	Moment
M_u	Ultimate moment
P	Mid-span load
RC	Reinforced Concrete
TRC	Textile Reinforced Concrete

Roman lower case letter

a	Longer distance from load application point to support
b	Shorter distance from load application point to support
b_{slab}	Slab's width
c	Concrete cover
d_s	Distance from the top of the slab to textile layer
d_t	Distance from the top of the slab to the bottom steel reinforcement
f	Ordinate value of modified Thorenfeldt's curve
f_{cc}	Compressive stress
f_{cf}	Compressive stress function
f_{cm}	Compressive strength
f_p	Peak stress value

f_y	Yield stress of steel reinforcement
h	Height of the slab
k	Parameter in Thorenfeldt's curve
l	Span of the slab
n	Parameter in Thorenfeldt's curve
q	Total self-weight
$q_{concrete}$	Concrete self-weight
q_{TRC}	Textile reinforced concrete self-weight
u	Mid-span deflection
$u_{self\text{-}weight}$	Mid-span deflection caused by the self-weight
x	Height of concrete compressive zone
x'	Corrected height of concrete compressive zone
z_s	Internal lever arm of steel reinforcement
z_t	Internal lever arm of textile reinforcement

Greek letters

α	Strain in Thorenfeldt's curve
α_p	Modified peak strain
$\beta_{\varepsilon_{cr}}$	Strain coefficient
$\beta_{\sigma_{cr}}$	Stress coefficient
ε	Strain
ε_c	Concrete strain
ε_p	Peak strain
ε_s	Steel strain
ε_p	Textile strain
σ	Stress
σ_{bond}	Bond stress
σ_c	Concrete stress
$\sigma_{concrete}$	Concrete stress
$\sigma_{textile}$	Textile stress
ρ	Density
χ	Attenuation coefficient

1 Introduction

1.1 Background

Concrete has been used effectively since ancient times. In the middle of 19th century Reinforced Concrete (RC) was invented and was greatly influential in the development of new structures (Bosc et al, 2001). As a result, RC became a very popular material and nowadays most constructions are made of this composite material. Despite its popularity, RC structures do pose some disadvantages, which are related to durability and corrosion of reinforcement. To avoid such deterioration, sufficient cover layer is needed. In some cases this could lead to a significant increase in self-weight. For example, the rehabilitation of slabs using RC could have a big influence on the self-weight of the final structure.

Approximately over one decade ago, researchers had the idea of replacing the steel reinforcement with alkali-resistant fibres. These high-resistance materials like glass, carbon and aramid were used to produce these fibres and resulted in a product called Textile Reinforced Concrete (TRC), see Brameshuber (2006). This new concept offers important advantages such as resistance to corrosion and thinner and lighter structures compared with traditional RC structures. These attributes enhance the overall design of new constructions.

In rehabilitation one can utilize TRC to strengthen different structural elements such as slabs, beams or columns. Because of its high tensile strength and resistance to corrosion, TRC can be applied in layers much thinner than possible with RC and thus the overall weight of the rehabilitated structure is reduced.

Until now, there are very few established laboratories which are dealing with TRC. The biggest part of research has been undertaken with experimental testing, analytical and numerical modeling. Currently, there are two centers in Germany which are leading the research about this topic. One of them is "Textile Reinforced Concrete (TRC) – Technical Basis for the Development of a New Technology" at RWTH Aachen University and the other is "Textile Reinforcements for Structural Strengthening and Repair" at Dresden University of Technology.

Although TRC has been extensively investigated over the past decade or so by these research centres, there remains much to discover and define regarding its applications, production, structural design, mechanical and structural behaviour, bonding characteristics, durability, as well as life cycle.

1.2   Objectives

The main objective of this Master's Thesis is to model and analyse the effects of strengthening RC structures using TRC layers. The study particularly focuses on the modelling of a TRC strengthened RC slab in DIANA FX+ software. A secondary objective is to validate the developed model by means of experimental and numerical results from literature. An investigation of the sensitivity of critical modelling parameters is also included. Lastly, the applicability of this state-of-the-art strengthening method in new and existing structures is discussed in this study.

1.3   Methodology

The main method used in this project is numerical modelling based on the Finite Element Method (FEM). The finite element software DIANA FX+ was utilized to develop a 2-D non-linear model of a TRC strengthened RC slab. The verification of the developed model was accomplished by means of experimental and numerical results from a previous study. Thereafter, the sensitivity of critical modelling parameters was evaluated.

1.4   Limitations

One of the main limitations which exists in this project is the fact that experimental testing was not possible during the time of this study and due to this reason, experimental results from literature was used for model verification.

As such, these experimental results dictated the characteristics of the present model (i.e. shape, loads, material properties, boundary constraints, bond slip behaviour, etc.), as well as the researched failure type of bending.

Another limitation is that the shear behaviour was not investigated as only bending failure is focused on in the developed model. This aspect is due to the outcome of the experimental results, where all specimens were observed to fail in bending (e.g. fracture of textile layers). It should be noted, however, that no bond failure (e.g. delamination) was observed in the results. Bond slip behaviour between the reinforcement and the concrete matrix were taken into account in the modelling.

2 Textile Reinforced Concrete

An alternative strengthening material that has become of interest as of late is Textile Reinforced Concrete (TRC). This state-of the art composite material can be used in new structures, as well as in strengthening of beams, slabs, columns and even walls. It is of particular interest to discuss TRC as a strengthening material in this study.

Some alternatives to TRC as a strengthening solution, are the so called Fibre Reinforced Concrete (FRC). In FRC, the principle is to insert short fibres in the concrete matrix. These fibres could be metallic (steel), mineral (glass), natural (cellulose, Jute, etc.) or polymeric (acrylic, aramid, carbon, nylon, etc.), according to Davis (2007). One important difference between TRC and FRC is that the short fibres in FRC are oriented in all directions, when the textile fibres in TRC behave like a normal steel reinforcement, with the exact orientation to support the efforts. This results in higher strengths for TRC than in FRC.

Another advantage of TRC in comparison with RC is that the reinforcement, the fibre mesh, is lighter and easier to work with. One can work with the textile mesh easily, bend it by hand or use it to wrap structural elements such as beams or columns. In comparison with working with the steel reinforcement bars, TRC is easier to work with and provides a rapid application on elements which are not strengthened.

A description of TRC is given in this section. Firstly, the type of fibres, concrete matrix and technologies of production are presented. Thereafter, mechanical behaviour, durability and bond behaviour are discussed. The applicability of TRC as a strengthening solution is explored in the end.

2.1 Textiles

2.1.1. Applicable materials

Textile fibres have a great influence on the strength of composite materials, their properties as well as their magnitude. Materials which are most applicable for use in TRC structures are alkali-resistant glass (AR-glass), carbon and aramid fibres. Besides the aforementioned materials, basalt, steel and polymers fibres can also be used. Steel fibre yarns are however not economically feasible and are thus not exploited (Brameshuber, 2006).This project will particularly focus on the carbon fibres, because they were used in the referenced experimental testing of the slab conducted by Schladitz et al (2012). The reason why the carbon fibres were preferred relies on their superior tensile strength, which is more appropriate for testing a full-scale slab. As such, this allows the research to come closer to reality.

2.1.1 Types of yarns

Textile reinforcement is composed of fibres constructed into yarns. The fabrication method and applied size (i.e. fineness of yarn) have a significant influence on the interaction between the filaments (i.e. adhesion) (Brameshuber, 2006). Thus, the mechanical properties of a fibre filament decrease when in the form of a yarn.

Yarns can be fabricated in various forms: filament yarn, bundled or twisted yarns and foil fibrillated tape, as illustrated in Figure 1. For reinforcing applications, filament yarns are preferred as they present smaller structural elongation (Brameshuber, 2006).
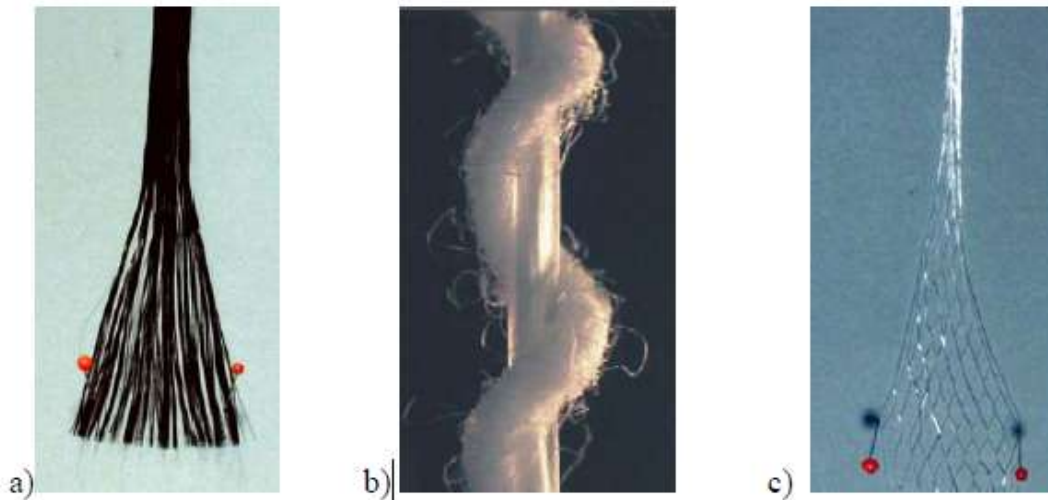
Figure 1   Types of yarns: a) Filament yarn b) Bundled yarn c) Foil fibrillated type (Brameshuber,2006).

The most common filament yarns used in TRC, namely AR-glass, carbon and aramid, are compared below in Table 1.

Table 1   Comparison of most common filament yarn types (Brameshuber, 2006)

	Diameter range (µm)	Density (km/m³)	Tensile strength (GPa)	Young's modulus (GPa)	Advantages	Disadvantages
AR-glass	9 to 27	2800	1.4	70 to 80	Very good adhesion to concrete	Low tensile strength
Carbon	7	1800	2 to 5	200 to 450	Superior tensile strength	Expensive
Aramid	12	1400	3	60 to 130	Low density Low brittleness	Negative heat expansion Low resistance to alkali attacks

It is clear that these fibres have great strengthening capacity. Their high tensile strength and their good resistance to corrosion, for example, make them a good choice for a reinforcing material. Despite the fact that they remain expensive and present some challenges in regards to production, these fibres nevertheless are plausible alternatives to traditional steel bars or short fibers.

2.2 Concrete matrix

The concrete used for TRC needs to fulfil demands, mechanical properties and durability, which are necessary to get proper composite material behaviour. Usually the maximum grain size used is less than 2mm, thus the concrete matrix is also called fine-grained concrete.

Matrix composition should have chemical compatibility with textile reinforced materials, consistency for full penetration, planned production process and mechanical properties for load-carrying capacity of a TRC element.

2.3 Mechanical behaviour of TRC

Within TRC the filaments are longer and placed in the direction of tensile stress. In this way, the fibres are used efficiently and the structure is optimised. Therefore, the load carrying capacity is increased and could in turn reduce costs.
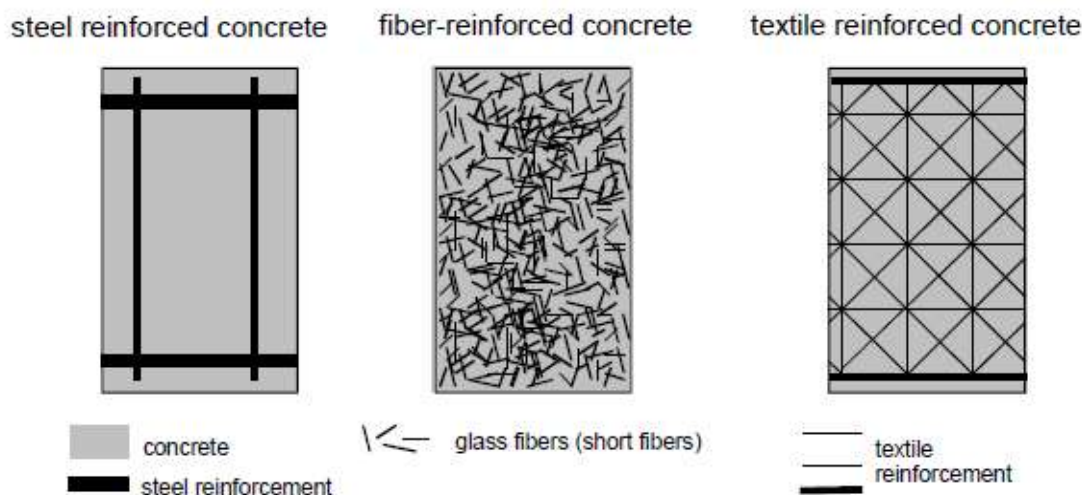

Figure 2   Reinforcing system of concrete (Brameshuber, 2006)

Load bearing performance and deformation behaviour have been investigated until now. Because of the low tensile strength of concrete, cracks will appear systematically. What is particularly important for all composite materials is not only the quality of the used materials, but also the bond behaviour of the reinforcing material. Even the shape of filament mesh has a significant influence on bond behaviour.

When all cracks appear, the tensile stress in the cracked cross-section is carried by the filament yarns. Depending on the layout of filaments, bond stiffness can be higher or lower, as such exact transfer lengths should be used. The most common aim of investigations is to find a model which can describe different bond characteristics of TRC.

2.3.1 General load-bearing behaviour

The load bearing behaviour can be analysed through various experimental tests such as compressive tests, tensile pull-out tests, and the classic bending tests. These experiments give a good understanding of the load bearing behaviour of TRC, and also provide key material properties: compressive strength, tensile strength, stress-strain behaviour, and bond-slip behaviour. The stress-strain diagram of TRC is similar to conventional Reinforced Concrete (RC), as illustrated below in Figure 3.
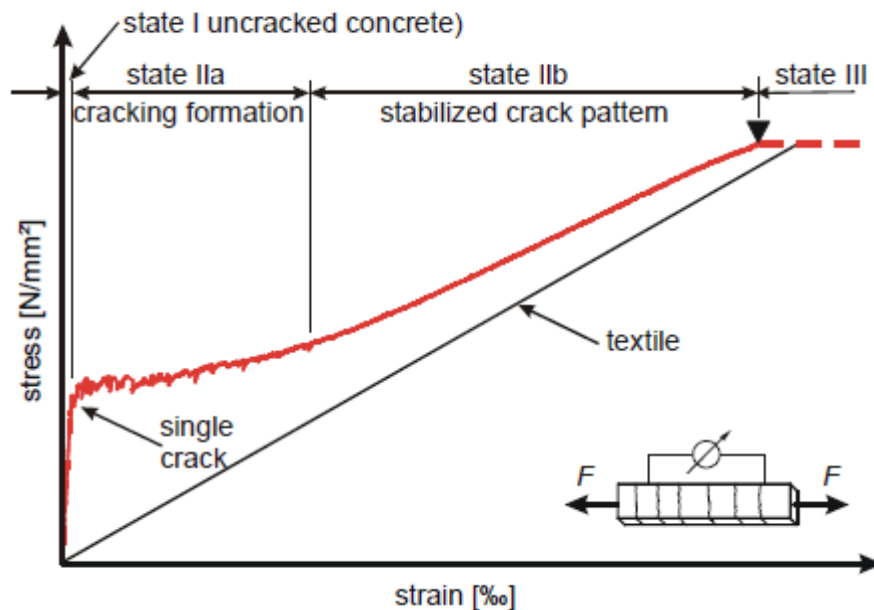

Figure 3   *Stress-strain diagram of textile reinforced concrete under uniaxial loading (Brameshuber, 2006)*

As is shown in Figure 3, at the beginning of loading, the stiffness of the composite material is corresponding directly to the E-modulus of fine concrete (i.e. State I). When tensile strength of concrete is achieved, the first cracks occur. All the tension in the cracks is carried by the reinforcing material. It means that this material should be strong enough not to lead to the failure of the fibre mesh. After increasing tension force, additional cracks appear (i.e. State II a). Crack widths and cracking distance are determined by reinforcement and bond characteristics. During the appearance of the multiple cracking the stress-strain curve reveals a low increase. Stabilising crack pattern is achieved in State II b, and after this state no more cracks occur.

Before the tests started (Hegger, 2004), the expectations were to achieve the same stiffness for TRC at the State II b as the Young's Modulus of the textile fibre alone. Unfortunately in most tests, the TRC's stiffness was about 10 to 30 % lower. The stress-strain curvefor a composite material progresses almost parallel to the stress-strain curve of pure textile. The difference is explained by tension stiffening effect. Since AR-glass and carbon materials have no plastic capacity, the ductile deformation area (i.e.State III) does not appear in the tensile test of TRC. Hence, the TRC is not a ductile material. Failure of composite material occurs when reinforcement reaches the tensile strain in a brittle manner.

2.4   Durability

The study of durability concerning TRC is relatively new compared with FRC, which has been the subject of considerable academic and commercial concern for the last 30 years. However, studies show that the problems related to durability are similar in TRC and FRC according to Brameshuber (2006).

Analysing the durability of FRC or TRC is a very complex process because many variables have to be taken into account. For example the bond between the fibres and the concrete matrix is conditioned by the chemical treatment of the fibres, the type cement used, and its behaviour in time is strongly related to these aspects.

One big advantage related to durability is TRC's resistance to corrosion. This aspect becomes important when, for example, a financial analysis is made in the conceptual phase. Even though TRC still is a fairly expensive option, durability and maintenance aspects are certainly not to be ignored.

Most common application is to use TRC for rehabilitation, however bridges made of pure TRC exists, as the pedestrian bridge done in Dresden, Germany in 2005 (Brameshuber,2006). Approximately seven years of tests and observations indicate only a beginning of the lifetime which is expected, but conclusions about durability are yet to be revealed.

2.5   Bonding behaviour of TRC

Many studies were dedicated to the bond behaviour within TRC. It is very important to completely understand the interaction between the textile fibres and the fine grained concrete, in order to foresee the behaviour of the entire structure, and eventually its failure.

In the process of strengthening RC structures with TRC, the bond between the old concrete and the new fine-grained concrete is also analysed according to Ortlepp et al (2006).

The interface between textiles fibres and concrete can be described using bond-slip diagrams. These diagrams are the result of different tests, the most popular one being the pull-out test. In this kind of tests, uniaxial tensile loading is applied to TRC specimens, and the shear stress as well as the slip are analysed. For more details, refer to Häussler-Combe et al (2007).

This project focuses on the analysis of RC slabs strengthened with TRC. In order to have realistic results, the interaction between the reinforcement and the concrete body needs to be modelled using a bond-slip diagram.

2.6   Applications of TRC

TRC can be used in a very large variety, in new structures as well as in strengthening and rehabilitation purposes.

Firstly, TRC can be used as a non-bearing element in:

- facade panels

- parapet sheets
- wastewater treatment plants
- noise protection wall systems
- water protection wall systems
- basement sealing
- exterior insulation systems

Secondly, the use of TRC includes some load bearing applications, such as:
- textile reinforced bridges, see Brameshuber (2006) and Groz-Beckert (2010)
- integrated formwork element for steel reinforced concrete floors
- integrated formwork element for steel reinforced walls
- balcony floor sheet
- diamond-shaped framework

In rehabilitation, TRC has proven high efficiency in strengthening structural parts of a building.

Due to its high tensile strength, TRC can be effectively used in strengthening elements in bending such as slabs or beams. By applying several layers of TRC at the bottom of the element which is strengthened, the resistance in flexural loading is substantially increased. For details, see Häussler-Combe et al (2007) and Bruckner (2006).

Also, by wrapping the core of the beams with layers of TRC, the shear performance of the entire structure is enhanced. Studies by Bruckner et al (2008) also include strengthening of columns using TRC.

Focusing on the strengthening of slabs, the method used is very simple: the bottom face of the slab is pre-wetted and roughened by sand-blasting and then the first layer of fine-grained concrete is applied. The application of this latter material can be effectuated by spraying or just by simple hand lay-up. The textile mesh is applied by hand on the fresh fine-grained concrete. This process of alternating fine-grained concrete and textile mesh can be repeated until the desired amount of reinforcement is applied under the surface of the slab. With this technique, the slab is strengthened with a small amount of concrete, which gives a small self-weight.

3 Test description

The tests chosen to validate the developed FEM model have been executed by researchers from Dresden Technical University in Germany. These tests and the analysis of their results are presented in Schladitz et al (2012). The reason why these particular tests were chosen is that they gave full details about the testing set up, and the results were validated by analytical and numerical analysis. Another advantage of these tests is the size of the tested slabs, which was comparable with the size of full scale slabs. This gives a realistic approach to the numerical model.

The purpose of these tests was to investigate the influence of TRC in strengthening RC slabs. Variation between different numbers of TRC layers was followed during tests, see Schladitz et al (2012). Due to the high degree of reinforcement of the slabs, a very good tensile strength was needed, so carbon fibres were preferred to glass fibres.

3.1 The strengthening process

For the experimental research five items of reinforced slabs were cast in the laboratory of Dresden Technical University in Germany, as described in Schladitz et al (2012). The TRC has the anticipated role of improving the bending capacity of the slabs, therefore it is applied in the critical points, where the tensile stresses have maximum values, at the bottom of the slab.

From a total of 5 RC slabs, one slab was kept unstrengthened as a reference and the other four were strengthened with 1, 2, 3 and 4 layers of TRC.
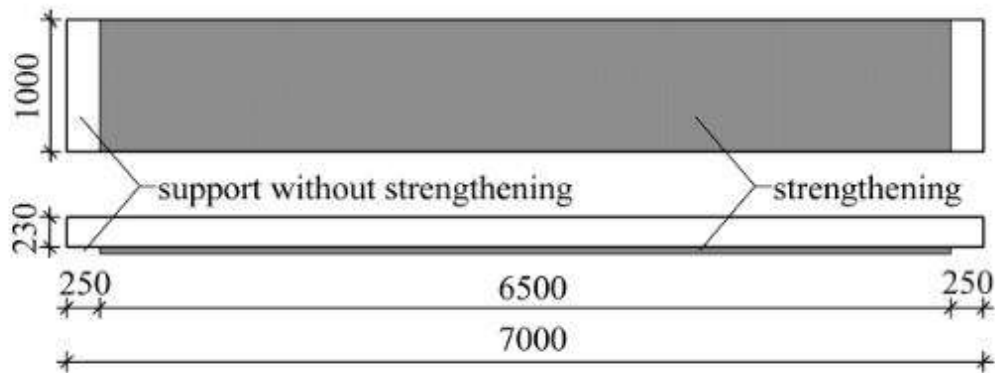

Figure 4   Application of TRC layers.

The application of TRC layers was done by hand lay-up, on the bottom face of the slabs, mounted vertically, as shown above in Figure 4. A layer of 3mm fine-grained concrete was applied by hand on the slab surface which was pre-wetted and roughened by sand blasting, Thereafter, the textile mesh alternating with the 3mm fine-grained concrete were applied according to Figure 5.

Normal concrete (RC slab)

Detail A

Fine-grained concrete

Textile reinforcement
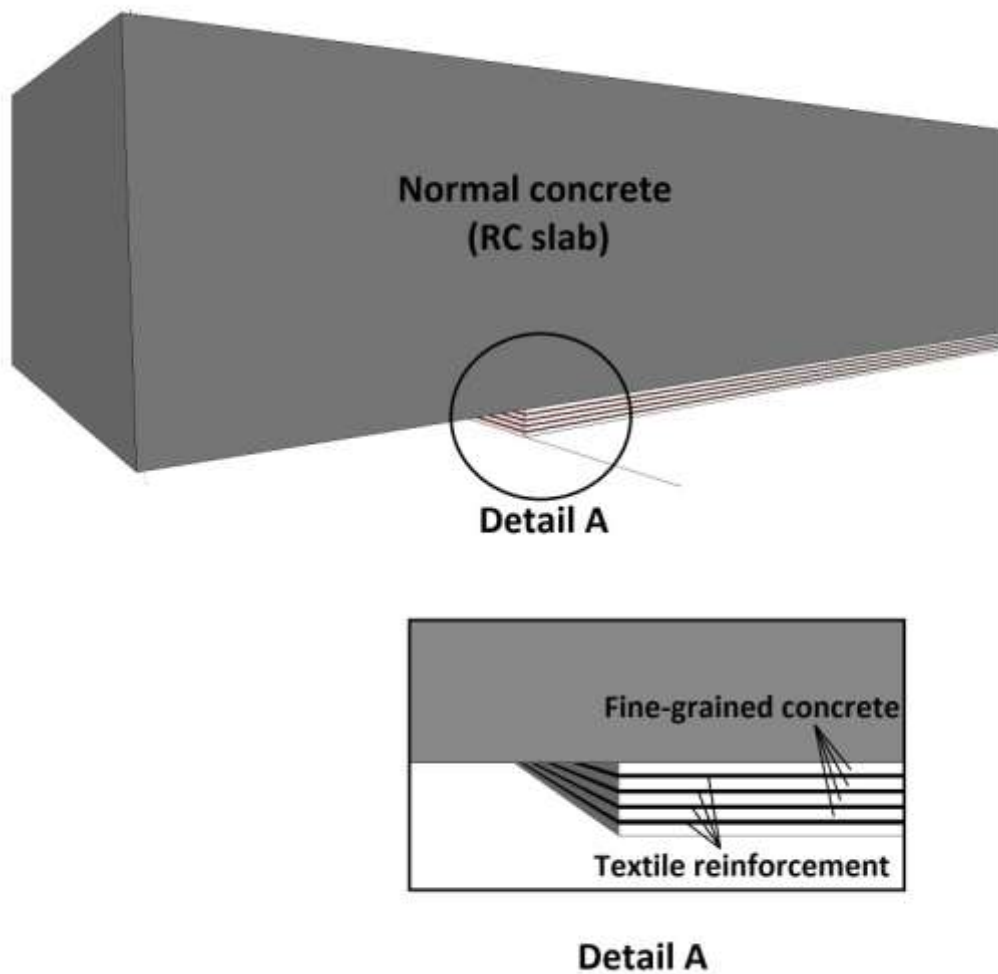
Detail A

Figure 5   The strengthening process, as used in tests (based on (Schladitz et al ,2012).

3.1.1   Testing setup

The specimens were 7m x 1m x 0.23m RC slabs which were simply supported at their ends. Two point loads were applied at an offset of 0.75 m from the centre of the slab. The span measured 6.75m, and the length of applied TRC was 6.50m, as depicted in Figure 6.
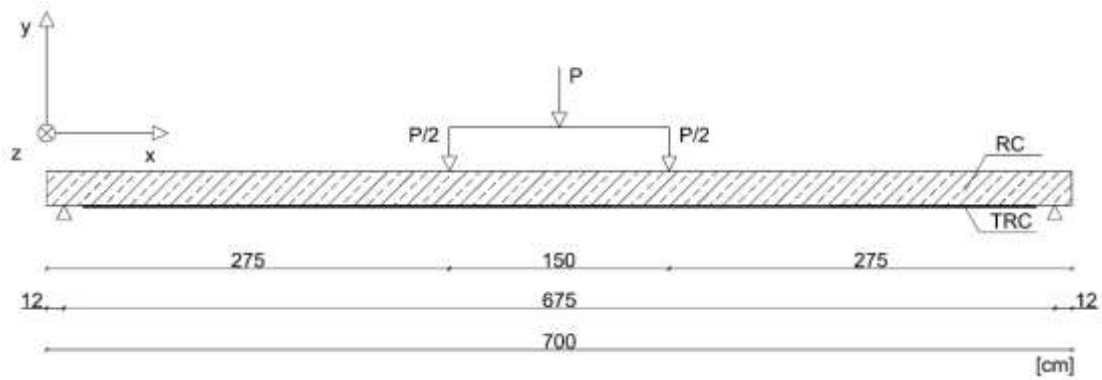
Figure 6 Sketch of tested slabs (based on Schladitz et al, 2012).

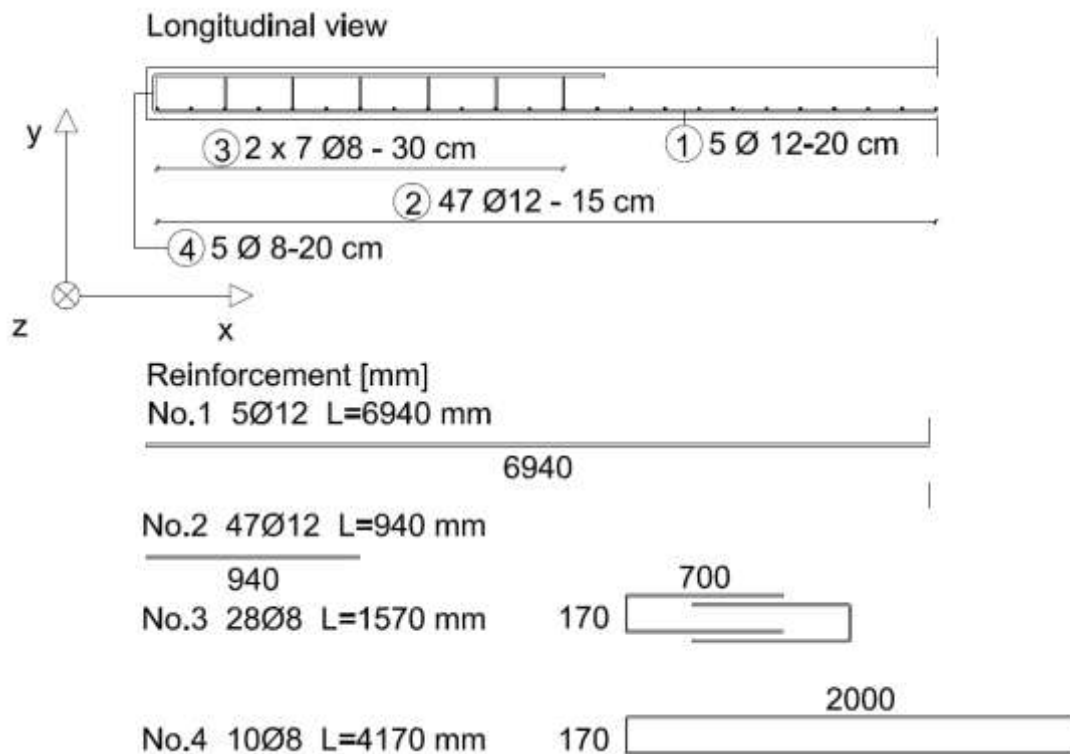The tested slabs had top and bottom steel bars, with stirrups, as presented in Figure 7.

Figure 7 Steel reinforcement of slabs used in experimental testing, (Schladitz et al, 2012).

The textiles used were so called heavy-tow-yarn carbon fibres, displayed in longitudinal and transversal direction, see Figure 8.
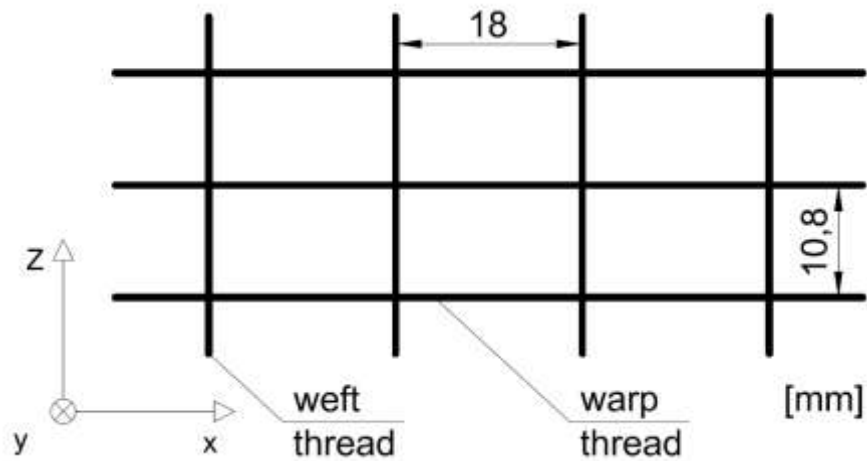
Figure 8   Textile mesh display, used in tests (based on Schladitz et al, 2012).

The RC slab, and also the slabs strengthened with 1, 2, 3, and 4 layers of textile were loaded until failure. The ultimate load and maximum deflection were precisely measured during the testing and graphically compared thereafter.

The purpose of the numerical modelling was to obtain results similar to the tests measurement and to approach real behaviour of strengthened slabs which give us possibilities for future modelling of constructions strengthened by TRC.

For full details about material properties and model characteristics used in the modelling refer to Chapter 4.

4 FEM model

The main part of this project was to create a valid model of a RC slab strengthened with TRC, using Finite Elements Method (FEM) analysis and DIANA FX+ software. The challenge relies in the fact that TRC is a relatively new and unknown material.

FEM has nowadays become an indispensable tool for calculating complicated structures. Using iteration methods to observe non-linear behaviour of materials, FEM gives much faster and more precise results than the traditional hand calculations, which are restricted to simplified calculations.

This chapter describes the analyses ran with TNO DIANA, version 9.4.3, and the pre and post processor FX+. This program allows a good non-linear analysis for concrete, bond-slip interactions and crack pattern analysis.

Analysis was carried out with deformation control instead of load control, which means that the force was replaced with deflection added stepwise. The reason for this type of loading was that deformation control analysis was more stable, and had easier to reach convergence. The whole demeanour needed to include not only a given applied force, P, replaced by deformation control, but also self-weight of the slab. One phase analysis was not sufficient to yield representative results, as such two phased analysis was needed. The first phase included the self-weight, as for the second phase, deformation was introduced at the location where the force P was applied.

4.1 General overview

A 2D model of the slab was developed in DIANA in order to analyse its behaviour under the four-point bending test, as previously shown in Figure 6. Firstly, the tested slab presented symmetric geometry and loading, therefore providing the possibility of modelling only half of it, as per Figure 9 below.
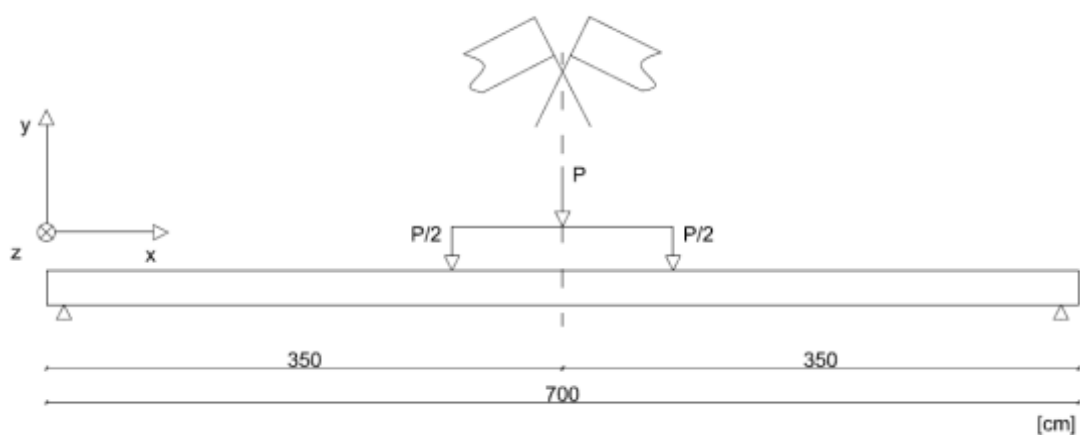

Figure 9   Symmetry used in the modelling.

The finite elements chosen for the concrete body were the 2D plane stress elements, called Q8MEM, as further described in DIANA (2010). This is a four-node

quadrilateral isoperimetric plane stress element. It is based on linear interpolation and Gauss integration, see Figure 10.
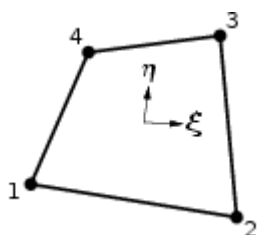

Figure 10   The plane stress Q8MEM element (DIANA, 2010).

Concerning the steel reinforcement, the transversal bars as well as the vertical stirrups were not considered in the numerical model because they were not relevant for the analysis of the slab in bending failure. Thus, only the longitudinal steel bars and the textile mesh were taken into account.

As aforementioned, the textile reinforcement in tests made by Dresden Technical University in Germany (2012) was applied in one, two, three or four layers with 3 mm of fine grained concrete between textile meshes. In the FE analysis, however, the separated layers were modelled by one layer and only material properties were modified. The placement of mentioned reinforcement was 10 mm from bottom of strengthening 15 mm layer, Figure 11. In the experimental tests, the slab body included the normal concrete and the layers of fine grained concrete which can reach at most 15mm. This homogenisation of the TRC layers into one layer was chosen to simplify the analysis and hand calculations proved that in the case of four separate textile layers or one equivalent textile layer the results were very similar, as further discussed in Section 5.1.
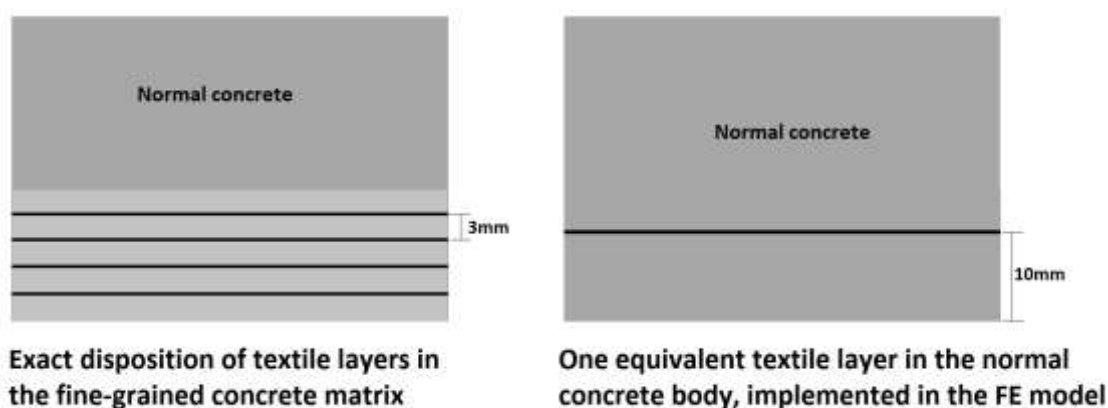

Exact disposition of textile layers in the fine-grained concrete matrix

One equivalent textile layer in the normal concrete body, implemented in the FE model

Figure 11   Implementation of the textile layer in the FE model.

4.2 Mesh

4.2.1 FE Model with Interface elements

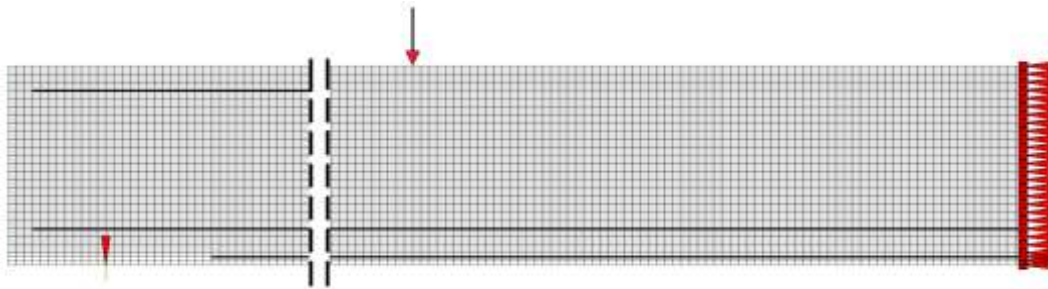Only the half of the slab was meshed as illustrated below in Figure 12.

Figure 12   Mesh in the FE model with interface elements.

The concrete body was meshed with four-point plane stress elements. The concrete mesh was divided in two regions: the upper part was constituted of 10 mm by 10 mm rectangular elements whereas the lower part is constituted of 10 mm by 5 mm rectangular elements.

The meshing of the interface elements was more complex, because the line interface elements and the steel or textile truss elements both needed to be placed in the same spot. This can be solved in DIANA FX+ in different manners. In this project the "convert element" option was chosen. This method works only if the line interface is placed over existent concrete nodes. In the lower part of the slab the textile reinforcement truss was inserted at 10 mm from the bottom of the slab.

4.2.2 Model with full interaction of the reinforcement

When considering the full interaction between the reinforcement and the concrete body, simple embedded truss elements were inserted in the proper place. This was possible with the option "bar in plane stress" in DIANA FX+. The implementation of embedded elements allowed a choice of homogenous mesh elements size. Therefore 17.5 mm by 17.5 mm rectangles were used, see Figure 13
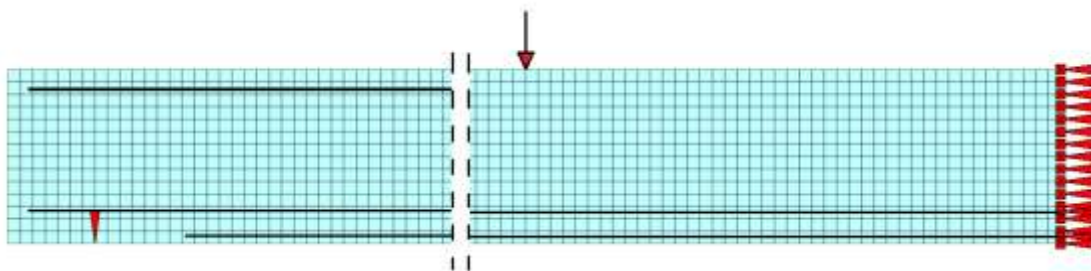

Figure 13   Mesh in the FE model with embedded reinforcement.

4.3   Boundary constraints

This model had two boundary constraints. The first one was representing the support, so the vertical translation was restrained. In order to create realistic conditions and to avoid local failure of the concrete, the support node was tied to some neighbour nodes using the option "eccentric tying" in DIANA. Also one beam element with "infinite" stiffness was created, connected to the point of support, see Figure 14. This element transferred the efforts to the neighbour nodes.

The number of nodes was chosen in order to represent the real supports. For example in the experimental tests executed by Schladitz et al (2012), the supports were approximately 8 cm wide, so eight nodes (four from the left side and four from the right side) were tied to the support node, see Figure 14.
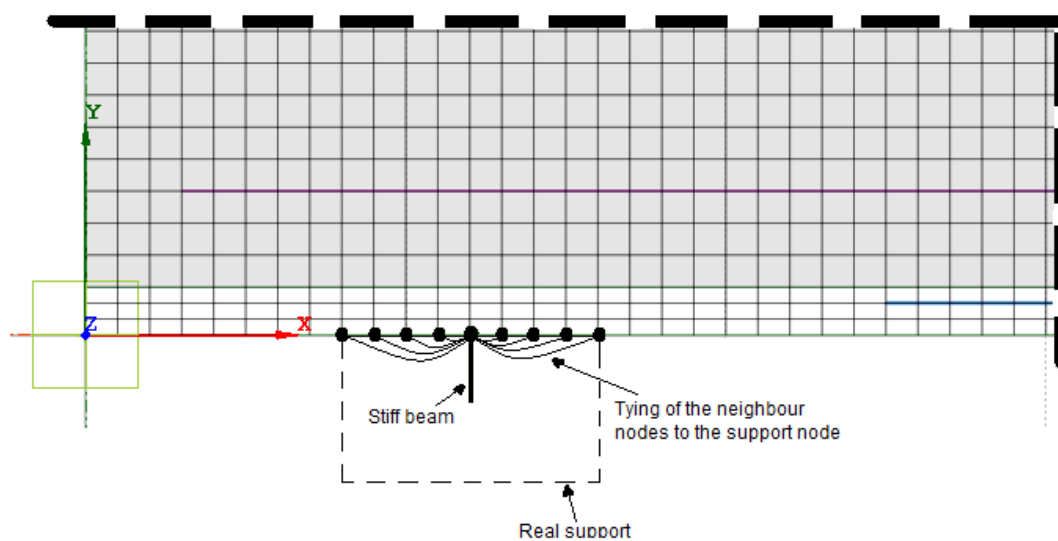
Figure 14   Eccentric tyings at the support of the slab.

The same method was used for modelling the point load, P, such that tyings were defined in order to avoid local failure of the concrete. It should be noted that the load was applied at the end node of the stiff beam connected to the concrete slab.

The second boundary constraint was at the middle of the slab, in this case at the end of the model. When using symmetry, the translation along the longitudinal and transversal direction as well as the rotations along transversal and vertical direction must be blocked. The plane stress element does not allow rotations as degrees of freedom, so finally only the translations in horizontal direction were restrained. Figure 15 shows the FE model of the slab and its boundary constraints.
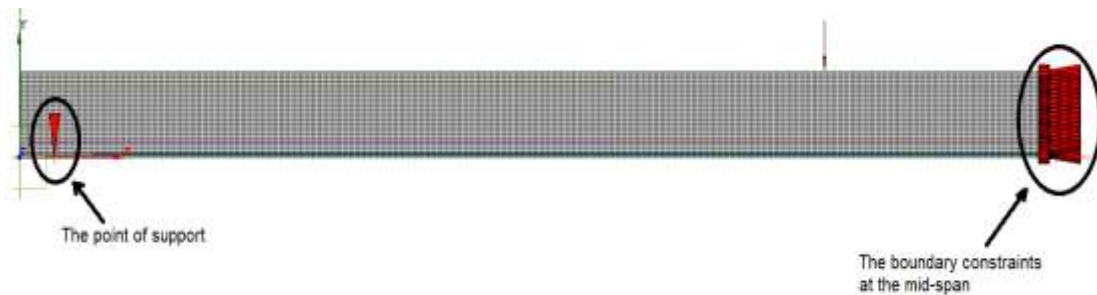
Figure 15   FE model with boundary constraints.

4.4   Materials

4.4.1   Concrete

The concrete used for the tested RC slabs had key properties, which were very important for the input of the FE Analysis. The maximum size of the grain was 16mm. The compressive strength and the splitting tensile strength have been determined on cubes (l = 150 mm) and they were equal to 45.5 MPa and 2.9 MPa, respectively. The compressive strength on cylinders, f_{cm}, was calculated according to CEB (2010), and its value was 38 MPa. The Young's modulus was equal to 26 150 MPa, determined on cylinders (Φ/h= 150mm/300mm).

As discussed in the previous section, the RC slab and the fine-grained concrete were modelled as one homogenous concrete body, with the properties mentioned above. Therefore, the thickness of the FE model of the slab remain at a constant value of 24.5 mm in all the five cases (unstrengthened, 1, 2, 3 and 4 layers of TRC).

The concrete was modelled as a homogenous and isotropic material. The model which was implemented in DIANA FX+ took into consideration the following effects of concrete behaviour:

- The behaviour in compression was modelled in two different ways in order to analyse their influence on the results: firstly the non-linear modified Thorenfeldt's curve was utilised, and then ideal-plastic behaviour was implemented. The influence of these two models will be further discussed in Chapter 5.

- The modification of the Thorenfeldt's curve was necessary, as shown in Figure 16, in order to take into account the size of the finite elements in the numerical model. Refer to APPENDIX B for calculations.
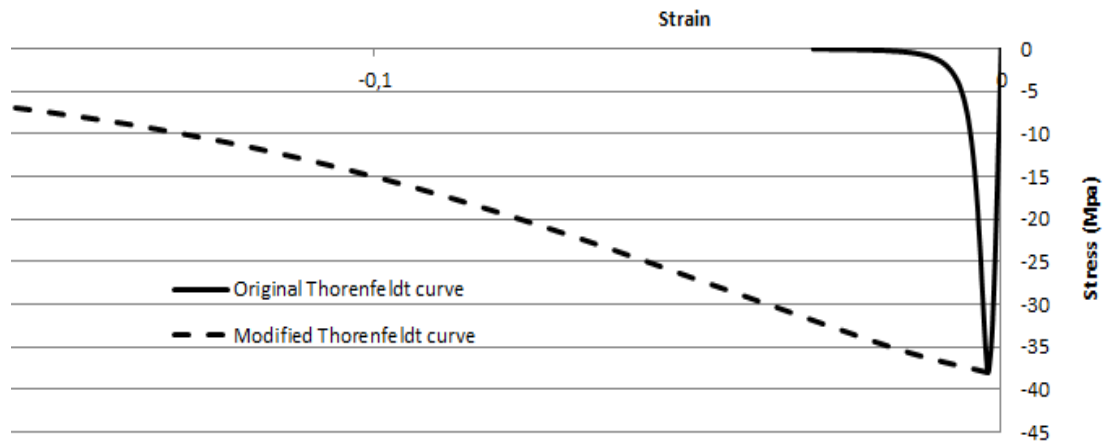
Figure 16   Original and modified Thorenfeldt's curve, (based on DIANA, 2010).

- Total strain rotating crack model was used, which describes the cracking and crushing behaviour of the material with a non-linear elasticity relationship. In this model stress-strain relationships are evaluated in the principal directions of the strain vector.

- The fracture energy in tension was calculated from the compressive strength according to CEB (2010). Thus, G_F was calculated to be 140.5 N/m.

- Tension softening was considered according to Hordijk's curve, see HORDYK input in DIANA (2010).
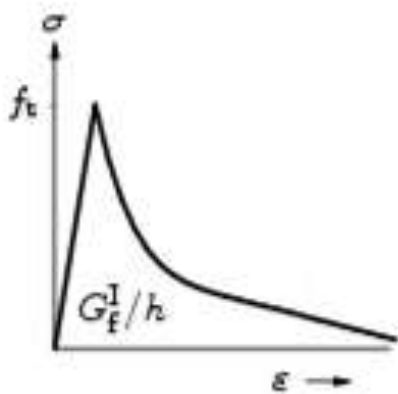
Figure 17   Tension softening according to Hordijk (DIANA, 2010).

- The softening curve was based on fracture energy by the definition of the crack bandwidth. For this crack bandwidth, DIANA assumes a value related to the size of the element. In this FE model, it was useful to specify the crack bandwidth explicitly by means of the CRACKB input item. The value of the crack bandwidth depended on the size of the mesh, as well as on the interface between the concrete and the reinforcement, and its value is further discussed in Chapter 4.3.

4.4.2   Reinforcement

Two types of reinforcements were modelled: steel bars and textile mesh. Both reinforcements were modelled as truss elements, namely L2TRU in DIANA. Their interaction with the concrete body was implemented in two different ways in order to analyse their influence on the results:

- Firstly, full interaction was considered, which means that the bond between concrete and reinforcement was assumed to be perfect and no slip was permitted.

- Secondly, interaction was modelled considering real bond behaviour, which was defined by a bond stress-slip-relation as per Figure 18. This relation was established using measurements from pull-out tests presented in Schladitz et al (2012).
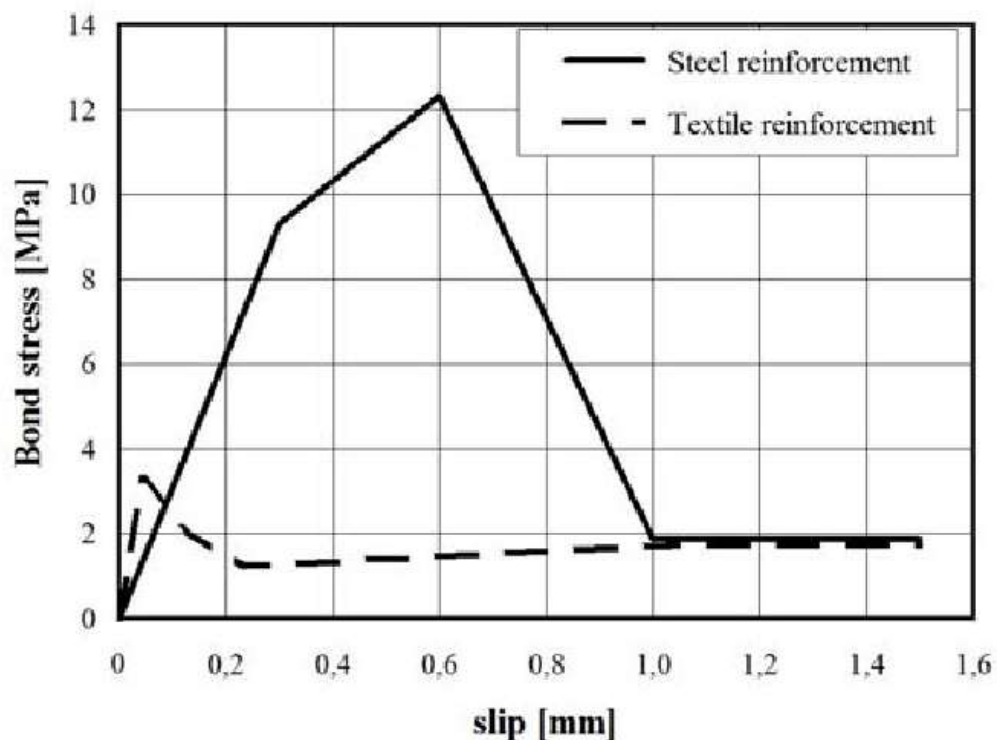
Figure 18   Bond-slip behaviour of reinforcement in concrete (Schladitz et al, 2012).

Another parameter which was implemented in the FE model with interface elements was the perimeter of contact for the textile mesh in the concrete matrix, which is described in Figure 19. This value was estimated as 0.5m in the model. The perimeter of one yarn was estimated from its cross-sectional area, assuming rectangular yarns. The transversal yarns were not taken into account. It should be noted that the value of 0.5 m was used in all analyses, regardless the number of layers; even though it was estimated from the perimeter of one layer of textile. This parameter has an influence on the bond-slip behaviour between the concrete and the textile reinforcement which is further discussed in Chapter 5.
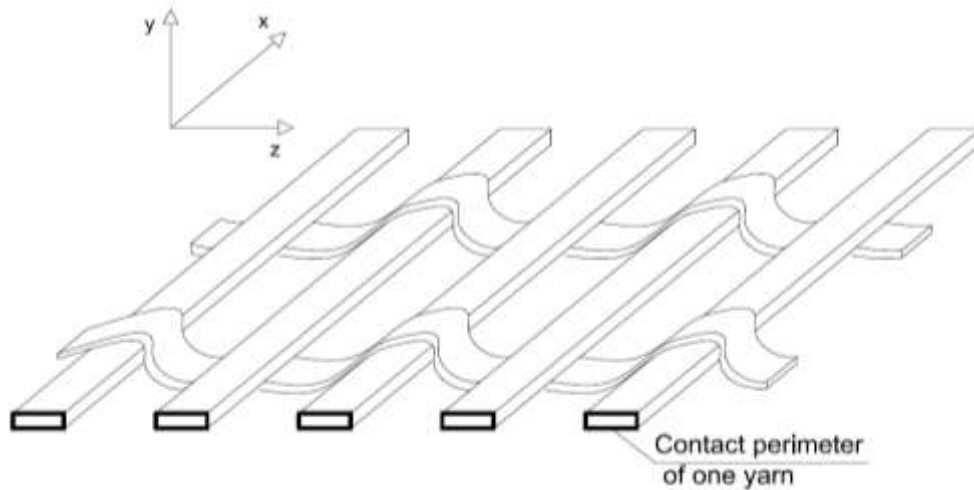
Figure 19   Contact perimeter of textile mesh

Only the top and bottom longitudinal steel reinforcement were chosen to be included in the FE model because the transversal bars as well as the stirrups were not relevant to the analysis of bending failure. The steel had an average yield stress of 574 MPa, and was implemented as a Von Mises material. A Young's modulus of 210 GPa was included. The implementation of ideal plastic behaviour for steel as per Figure 20 was found to be adequate.
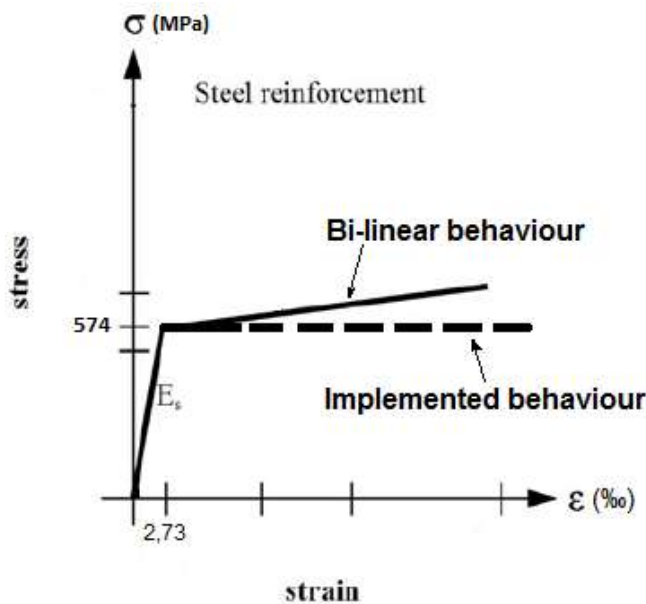
Figure 20   Stress-strain relation for steel reinforcement (based on Schladitz et al, 2012).

The textile mesh inserted in the fine-grained concrete was polymer-coated fabric made of carbon rovings called SIGRAFIL C30 T050 EPY produced by SGL Carbon SE company. The carbon yarn had a fineness of 3 300 tex, which signifies that one km yarn weighs 3 300 g. Its density was 1 800 km/m^3 and the heavy-tow-yarns were aligned with a distance of 10.8 mm and 18 mm in the longitudinal and transversal

direction respectively. The average tensile strength of the textile yarns was 1 200 MPa, with a failure strain of 12 ‰.

The stress-strain curve in Schladitz et al (2012) presented a bi-linear behaviour as shown in Figure 21. The carbon yarns seem to become stiffer after a certain strain is achieved. This can be explained by the fact that the yarns are made of thousands of carbon filaments which are not fully stretched or fully aligned before loading. After a certain stress is applied, all the filaments start to work properly and this explains the higher stiffness. In the FE model an ideal-plastic behaviour was preferred as indicated in Figure 21. For a failure strain of 12 ‰, the Young's modulus of textile reinforcement was equal to 100 GPa. This ideal-plastic behaviour was simpler to introduce into the model, and its linear-elastic phase was found to be a reasonable simplification.
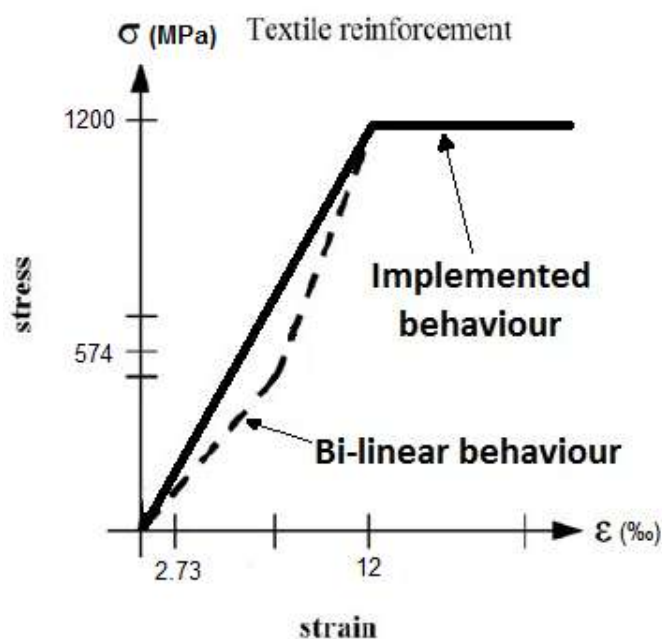
Figure 21   Stress-strain relation for textile reinforcement (based on Schladitz et al, 2012).

4.5   Processing

The solutions from numerical non-linear calculations in DIANA FX+, version 9.4.3 were based on two phase analysis as previously mentioned. The first phase included the self-weight and was applied as a body load in one single step. The second phase consisted of an applied deformation of 0.1 mm loaded to the slab at the position of the point load in the tests, with varying number of steps depending on the case considered. To reach proper results, the application node was supported in the *y*-direction, defined as TR2 in DIANA, before processing. This type of analysis is called deformation control, and was chosen for the analyses because it was more stable than load control and allowed for easier convergence in this given case. Lastly, Newton Regular was used as the iteration method in order to find equilibrium of each displacement increment.

5 Results

In this chapter, results from hand calculations, FE analysis, as well as experimental tests derived from Schladitz et al (2012) are presented. Moreover, a detailed comparison of these results is realised.

5.1 Hand calculations

Hand calculations were executed in order to obtain an initial behavioural prediction of the strengthened slab. Firstly, the initial deflection of the slab was calculated, and thereafter, calculations in the ultimate state were made. These calculations are based on considering full interaction between the concrete and both steel and textile reinforcements. The equations used in the hand calculations are described in APPENDIX A.

5.1.1 Deflection calculations

The initial deflection of the slab was calculated in order to analyse the behaviour of the slab in the non-cracked and elastic state. Due to its geometry, the slab is only one directional in bending, which means that its behaviour can be predicted with a beam approach. Firstly, the deflection caused by the self-weight, $u_{self\text{-}weight}$, was calculated to be 5.14 mm.

Secondly, the linear relation between the applied load, P and total deflection was established. Thereafter, the initial stiffness of the slab, K_{slab}, was calculated to be 5.4×10^6 N/m. This value is compared to the initial stiffness of the FE model in Section 5.2.

5.1.2 Ultimate moment calculations

The ultimate moments were calculated using simplified methods. The first simplification considers that the Navier-Bernoulli's hypothesis is accepted, meaning that the cross-sections remain planes and orthogonal to fibres after deformation. Furthermore, a rectangular stress distribution within the concrete compression zone is considered. The forces in steel and in textile were firstly calculated in the ultimate state and thereafter, the ultimate moment was obtained accordingly. These calculated values are summarized below inTable 2.

Table 2   Summary of ultimate moment calculations.

Parameter	Number of Strengthening Layers			
	1	2	3	4
Tensile Force: Steel, F_s (kN)	324.59	324.59	324.59	324.59
Tensile Force: Textile, F_t (kN)	211.20	422.40	633.60	844.80
Failure Moment of Slab, M_u (kN·m)	100.90	146.20	192.08	238.53

These values of the ultimate moments were compared to the experimental and FE model's results in Section 5.2.

5.2 FEM results

For the study of the RC slab strengthened with TRC layers, a multitude of FE analyses were ran in order to achieve comprehensive results. Figure 22 illustrate the number and the type of all analyses carried out in this project.
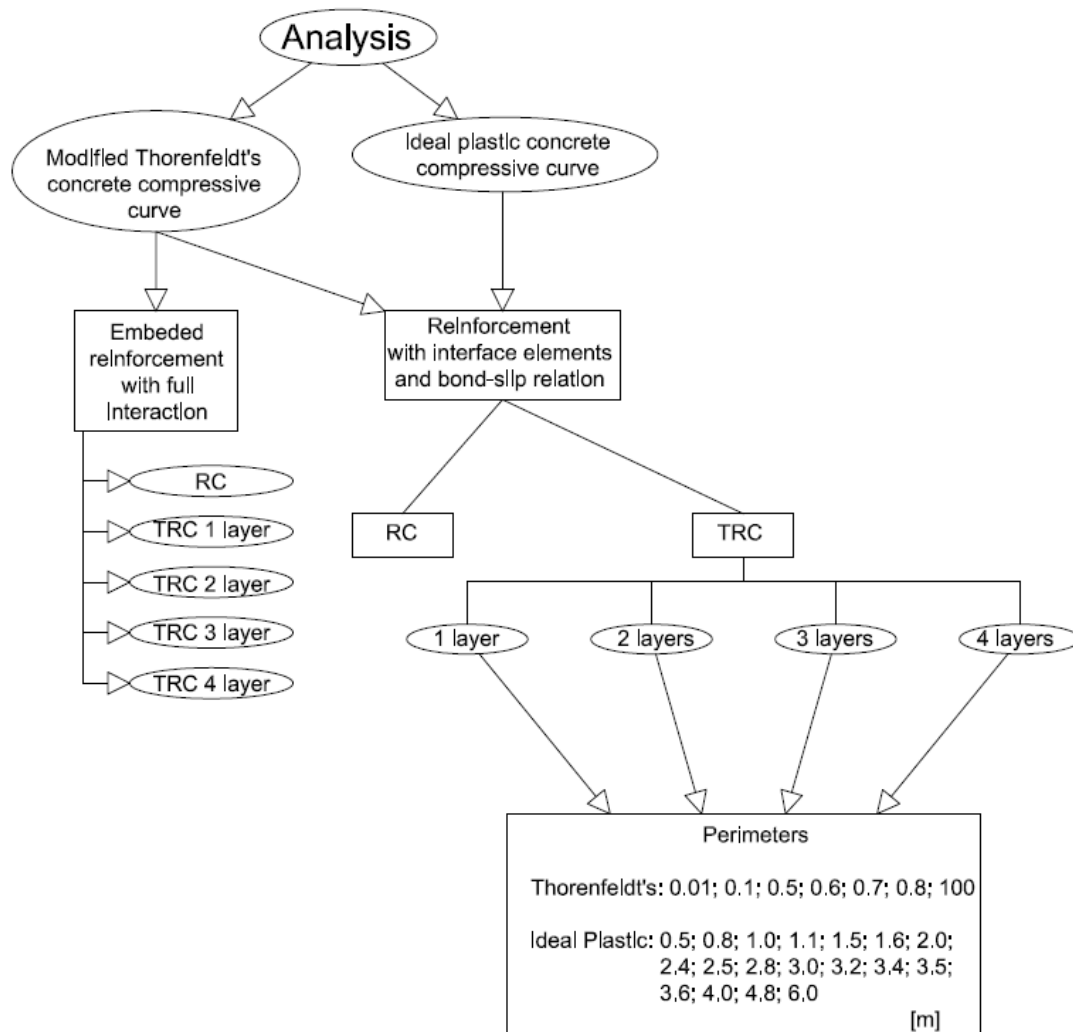
Figure 22   Flow-chart of the analyses carried out in the study.

As observed in Figure 22, the main variations incorporated in the analyses involve the concrete compressive curves and the reinforcement interaction. Furthermore, RC analyses were included as a benchmark to observe the strengthening effect of varying layers of textile reinforcement (e.g. 1-4 layers). Lastly, a parametric study of the influence of the textile perimeter was evaluated.

5.2.1 General overview

The main objective of this project was to model and analyse the effects of strengthening RC structures using TRC layers by means of finite element analysis. In this section, the results from FE analysis are presented and discussed in detail.

The FE analysis was carried out using two types of implementation for the reinforcement: embedded reinforcement with full interaction and interface elements with bond-slip relation. A comparison of the simulation results is presented in Figure 23 below. In all four cases of strengthening, the model with full interaction reinforcement has a larger stiffness during the loading process. This model did not allow any slip between the reinforcement and concrete, therefore the stiffness of the strengthened slab is overestimated in this case.
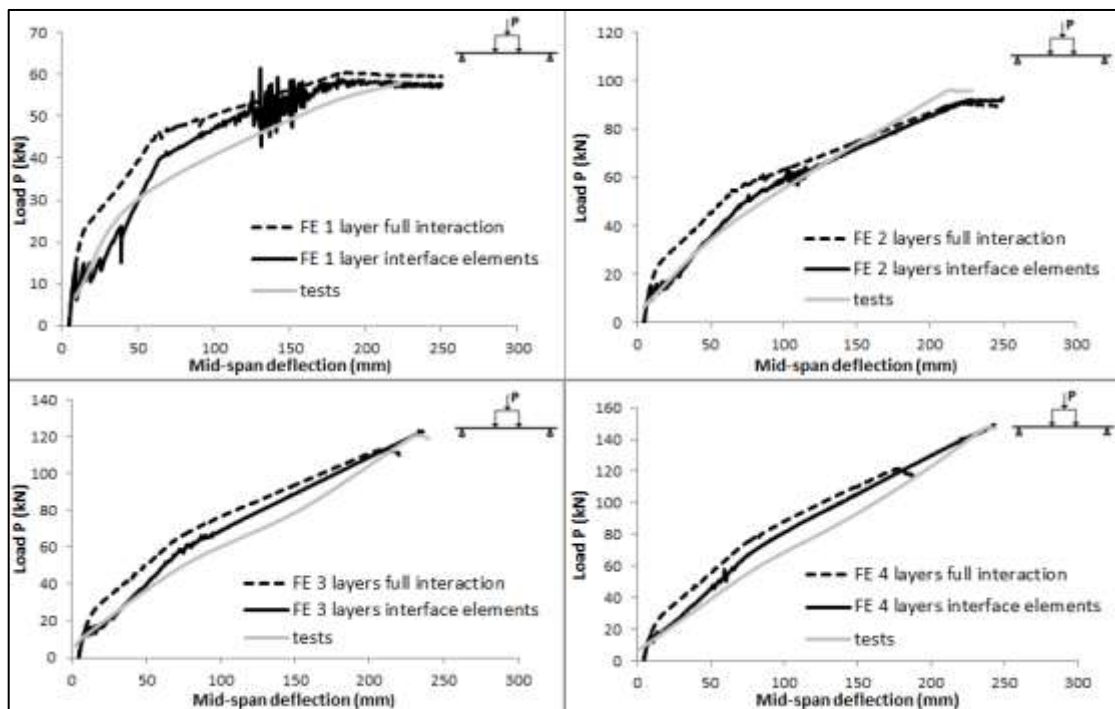
Figure 23   Influence of reinforcement implementation on load-deflection behaviour

It is observed in Figure 23 that the implementation of interface elements with bond-slip provided a more accurate correlation with the behaviour observed in the tests. For this reason, these models were chosen to be further investigated. Results from the models with interface elements for the RC reference and also for all four cases of strengthening are presented below in Figure 24. .
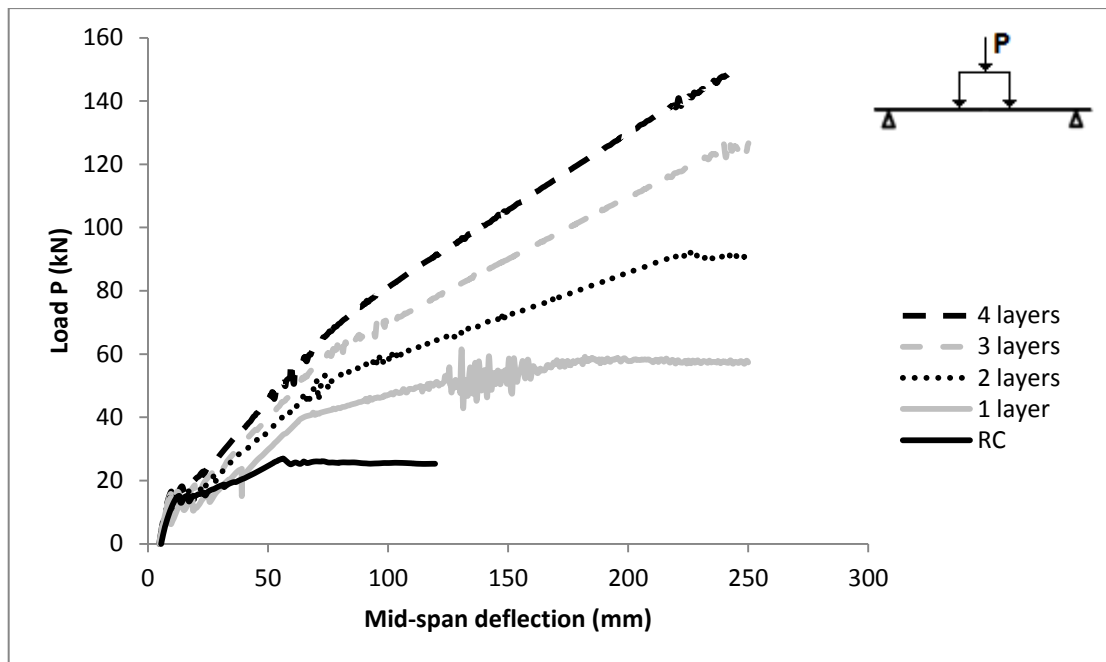
Figure 24   Comparison of FE analysis results.

Figure 24 shows the load-deflection behaviour of the RC slab in different cases of strengthening. It is apparent that with each layer of TRC the ultimate load increases consistently. Another enhancement of the strengthened RC slab is the deflection. At the same level of applied load, a high amount of textile reinforcement corresponds with a lower deflection. Therefore, the performance of the strengthened RC in the Service Limit State (SLS) is increased. The following table, Table 3, summarizes the improved load bearing capacity of the strengthened RC slab. The results of the numerical model conclude that the performance of the RC slab is enhanced when it is strengthened by TRC layers.

Table 3   FE results: improvement of the load bearing capacity.

Case	FE model	Improvement of the ultimate load
	Ultimate Load, P (kN)	Compared to reference (%)
RC (reference)	25.4	100.0
1 layer	57.8	227.6
2 layers	91.4	359.8
3 layers	122.8	483.5
4 layers	149.6	589.0

A secondary objective of this study was to validate the developed model by means of experimental and numerical results from Schladitz et al (2012). The results obtained from the FE model are compared to these experimental tests in Figure 25.
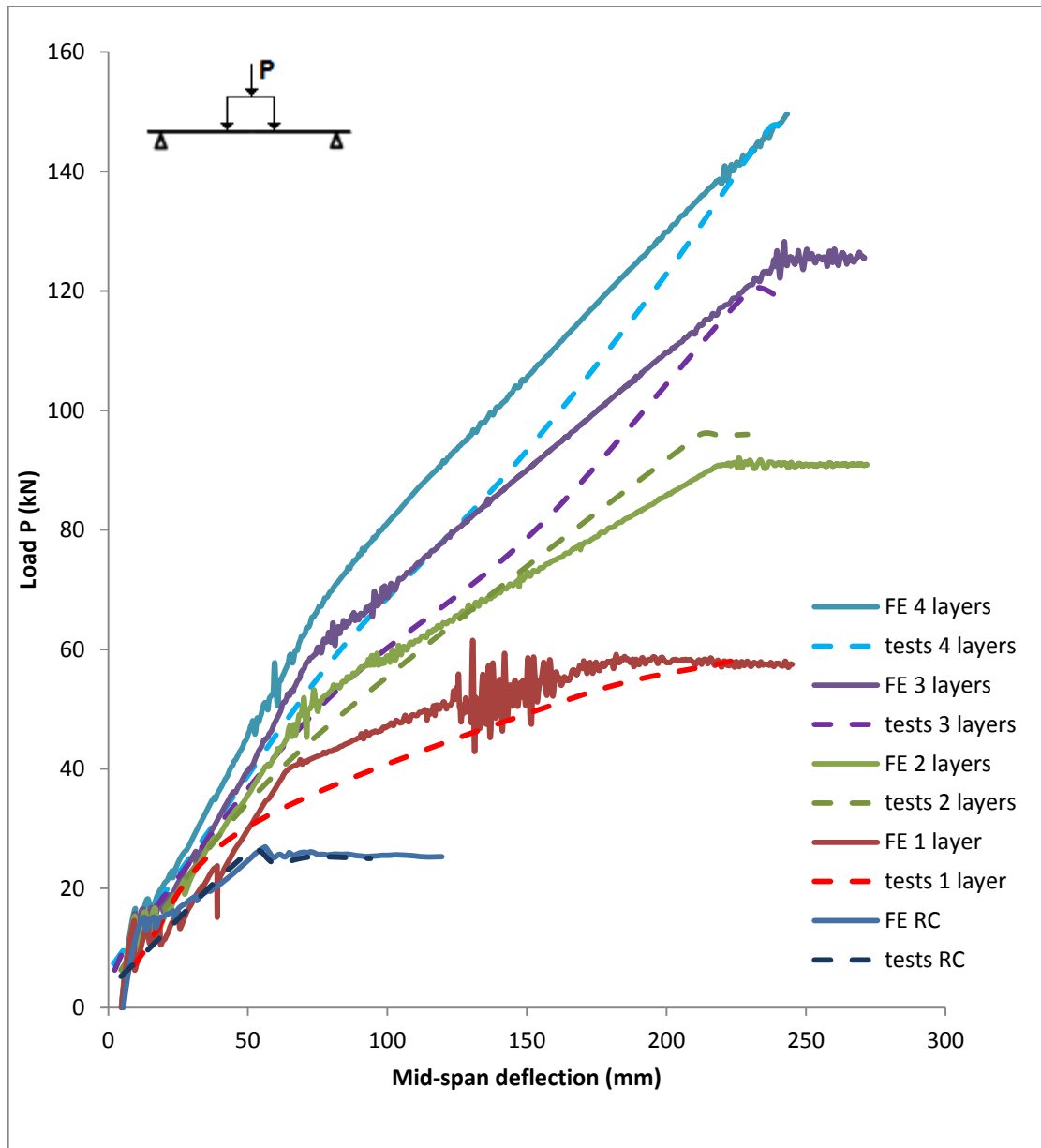
Figure 25   Load-deflection curves for FE model and tests from Schladitz et al (2012)

As observed in Figure 25, the ultimate loads obtained from the FE model correlate relatively good to those from the tests. A comparison between the ultimate loads is presented in Table 4.

Table 4   *Comparison of results from FE analysis and tests from Schladitz et al (2012).*

Case	FE model	Tests	Error (%)
	Ultimate Load, P (kN)		
RC (reference)	25.4	25.0	1.60
1 layer	57.8	58.0	-0.34
2 layers	91.4	96.0	-4.79
3 layers	122.8	119.0	3.19
4 layers	149.6	147.0	1.77

As Table 4 shows, the error of the ultimate load is small. However, the ultimate deflection is different. This discrepancy is explained by the implementation of the ideal-plastic behaviour of textile in the FE model, as per Figure 21. In reality the failure of the slab is observed by the brittle fracture of the textile layer. In the FE model, the failure is achieved when the textile layer has yielded. As such, the FE analysis was observed to converge for all demanded load steps.

Along the graphs slight deviations from experimental results can be observed. As Figure 25 shows, the stiffness of the model differs from experimental curves. The reasons of this variation rely on the choice made for the implementation of the FE model: the rotating crack model, the ideal-plastic behaviour of steel and textile, etc. These choices influenced the behaviour of the FE model.

In the FE model, the behaviour of concrete in compression was implemented firstly with ideal-plastic behaviour and secondly with modified Thorenfeldt's curve, refer to APPENDIX B. Although the results from these two implementations were very similar as Figure 26 shows below, the Thorenfeldt's curve was privileged because it considered a more realistic concrete behaviour, such that it took into account the softening of concrete. Therefore, all the results from the FE analysis presented in the above figures, Figure 24 and Figure 25, were achieved with the implementation of Thorenfeldt's curve.
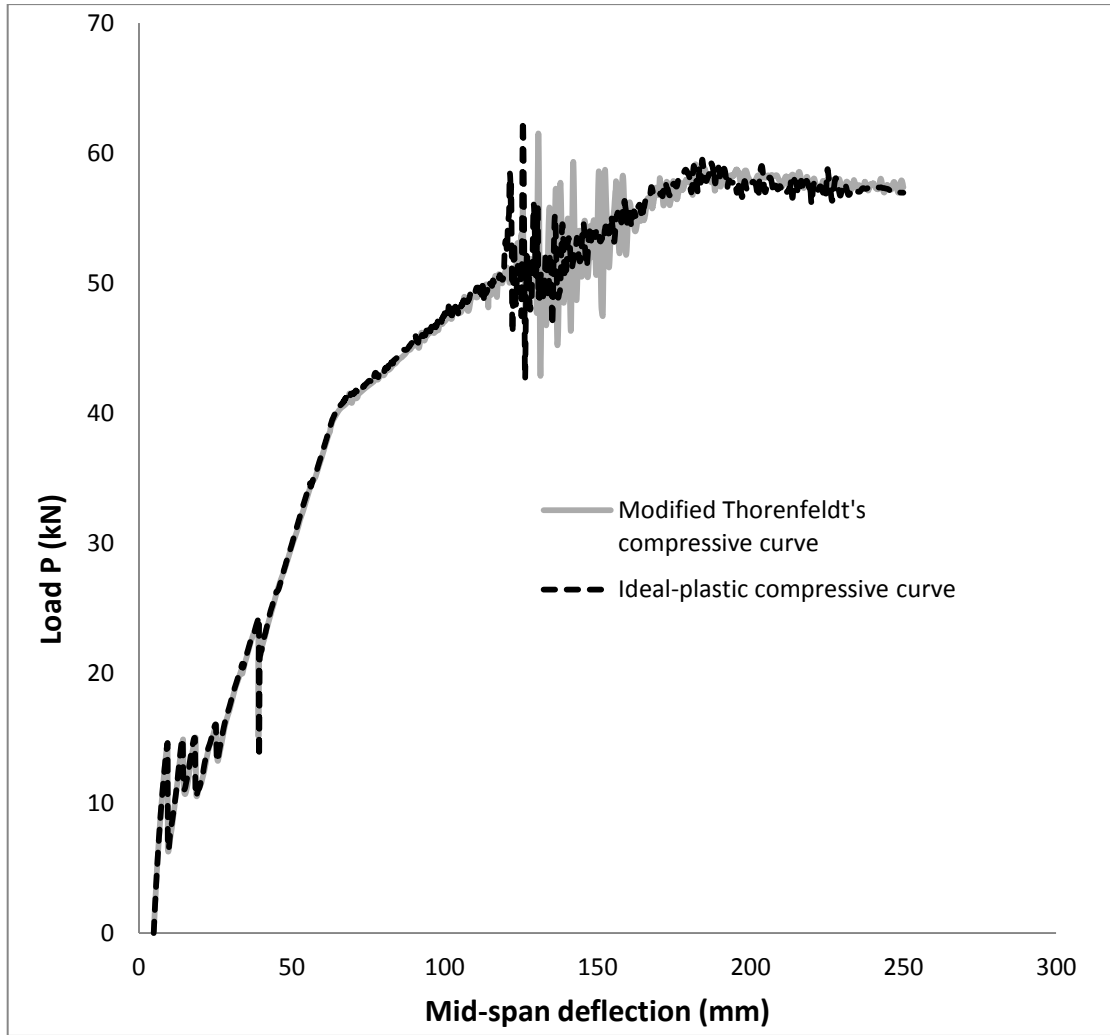
Figure 26   Influence of compressive curve on load-deflection diagram.

Furthermore, the FE results were compared with hand calculations. Firstly, as exposed in Chapter 5.1, the implemented FE model included one homogenous textile layer instead of four individual layers. The influence of this aspect on the results given by hand calculations is shown in Table 5 below:

Table 5   Hand calculation comparison.

Implementation Method	Ultimate moment (kN·m)			
	1 layer	2 layers	3 layers	4 layers
Hand calculations, individual layers	100.9	146.2	192.1	238.5
Hand calculations, 1 homogenous layer	101.2	146.4	191.5	236.7
Error (%)	-0.3	-0.1	0.3	0.8

The difference between the two ways of implementing the textile reinforcement is relatively small, which demonstrates the effectiveness of using only one homogenous textile layer in the FE model. The initial stiffness obtained by the hand calculations is also compared to the FE model results in Figure 27.
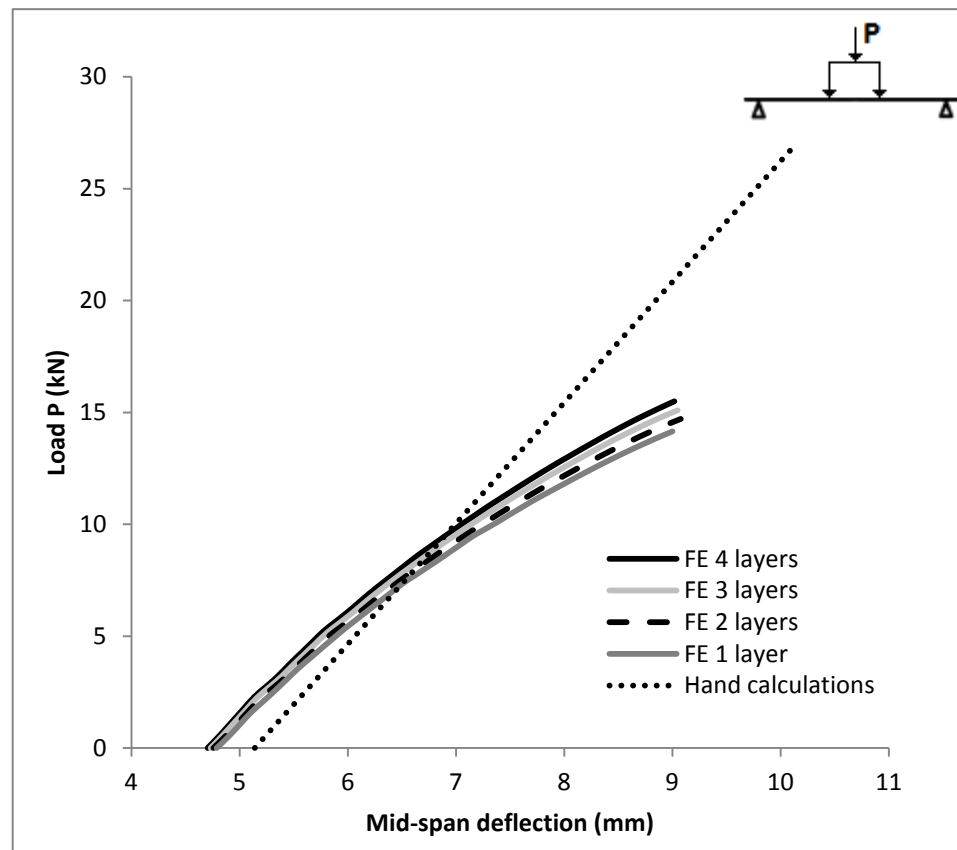
Figure 27   Initial stiffness of FE model compared to hand calculations.

Figure 27 shows that the hand calculations adequately estimate the behaviour of the slab in the initial phase of loading (up to 8% error), namely the uncracked state. In the FE model, the number of strengthening textile layers was found not to have an important influence on the initial stiffness of the slab. This behaviour was predicted by the hand calculations and is further described in APPENDIX A.

Hand calculations were carried out to estimate the load capacity of the slab in each case of strengthening. The comparison with the tests results is given below in Table 6.

Table 6   Hand calculations and FE analysis comparison.

Case	Ultimate Load, P (kN)		Error (%)
	Hand calculations	Tests	
RC(reference)	20.3	25.0	-18.8
1 layer	50.6	58.0	-12.8
2 layers	85	96.0	-11.5
3 layers	119.3	119.0	0.3
4 layers	153.8	147.0	4.6

Despite the fact that hand calculations consider full interaction between the reinforcement and the concrete body, Table 6 shows a reasonable estimation of the ultimate load.

5.2.2 Behaviour during the loading process

In this part of the study, the behaviour of the FE model was analysed, particularly focusing on the crack pattern, yielding of reinforcement and/or crushing of concrete. Moreover the failure modes were analysed in all FE models.

Initially, a model of the unstrengthened RC slab was created in order to have a reference for the strengthened models. The behaviour of this model was coherent with bending failure and the yielding of the steel reinforcement. The ultimate load achieved was in accordance with the hand calculations and tests results from Schladitz et al (2012). Detailed analysis of the behaviour of this FE model will not be presented, as this study focuses on the strengthened RC slabs, and the interaction between textile and concrete.

The first strengthening case to be analysed is the model with one layer of TRC. Its behaviour is presented in Figure 28. The commencement of the loading process presents an elastic phase with almost constant stiffness. Then, the first cracks in the concrete appear which is exposed by a sudden variation of the load (i.e.'bumps' on the graph). This process is followed by the stabilisation of the cracking and subsequently yielding of the bottom steel reinforcement. The stiffness of the slab is reduced and the steel continues to yield. After this state, the graph describes large oscillations of the load, and the steel yields. The stress in the textile reinforcement increases until the yielding point. At this stage, the ultimate load is achieved and the textile continues to yield. In the graph, this behaviour is characterized by nearly a horizontal slope. In reality, the textile reinforcement has a brittle behaviour, which means that the yielding point of textile is the failure point.
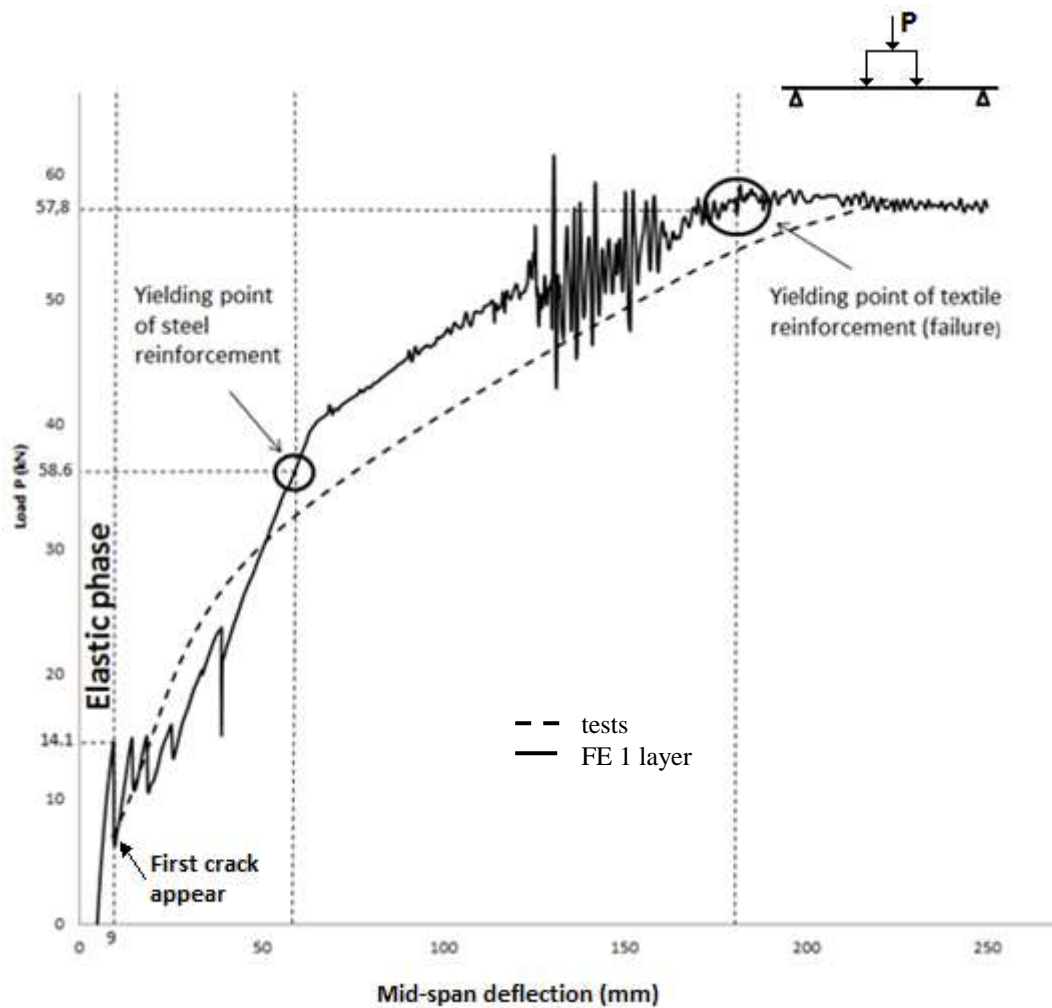
Figure 28   Behaviour of FE model (1 layer of TRC).

It should be noted that the 'bumpy' part of the graph between 120-160 mm of mid-span deflection is particular for the model with 1 layer of textile. The large variations of the load can be explained by instabilities in the analysis, with convergence being achieved after 15-20 iterations, more than in the other load steps. This instability does not occur in the other strengthening cases as can be seen from Figure 24.

Furthermore, the development of the crack pattern was analysed and is shown in Figure 29. It should be noted that the numbers represent the order of appearance of cracks. The cracks are in vertical disposition which is expected for bending tests and also indicates negligible shear effects.
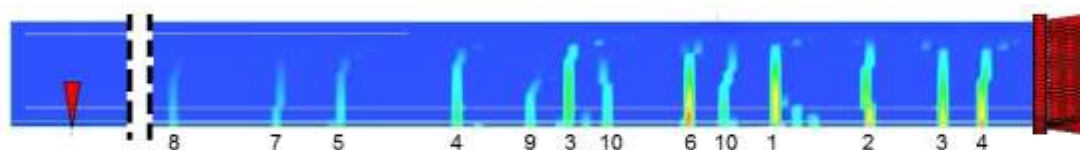
Figure 29   Crack pattern, 1 layer of TRC.

Moreover the models of the slabs strengthened with 2, 3 and 4 layers of textile reinforcement were analysed. As expected, their behaviour was very similar to the case of 1 layer of textile. The elastic phase is almost identical in all cases, as shown in Figure 27. Then, the same general behaviour was observed: crack appearance, yielding of steel, crack development and failure. The main difference was in the stiffness of the models and the ultimate load as observed in Figure 24. The model with 2 layers of textile had the same failure mode, the yielding of textile reinforcement. However, when 3 and 4 layers of textile were implemented, the analysis did not fulfil all demanded load-steps. Therefore, the yielding point of the textile layer was not reached, such that approximately 96% of yield stress was obtained. By designing one homogenous textile layer instead of separated layers, only the cross-section area of textile reinforcement was modified in each model (2, 3 and 4 TRC layers). The contact perimeter between the textile mesh and the concrete body, (see command THICK in DIANA and APPENDIX C), was kept constant in each model (i.e. 0.5 m). The influence of the contact perimeter is further analysed in Section 5.2.3.

5.2.3 Influence of the contact perimeter on the FE models

In order to understand why the analyses of the models with 3 and 4 layers of textile ended before the yielding of textile mesh, further analyses were ran with different values of the contact perimeter. The results of these later analyses showed significant change in the final load and final deflection. This observed influence of the contact perimeter lead to a parametric study. The study showed that for a certain value of the contact perimeter (i.e. 0.5 m), the analysis carried out more load steps and higher stress in the textile reinforcement was achieved. Figure 30 below indicates that in each model there is an optimum value of the contact perimeter. It is also clear that for larger perimeter values, the final load achieved is stabilised.
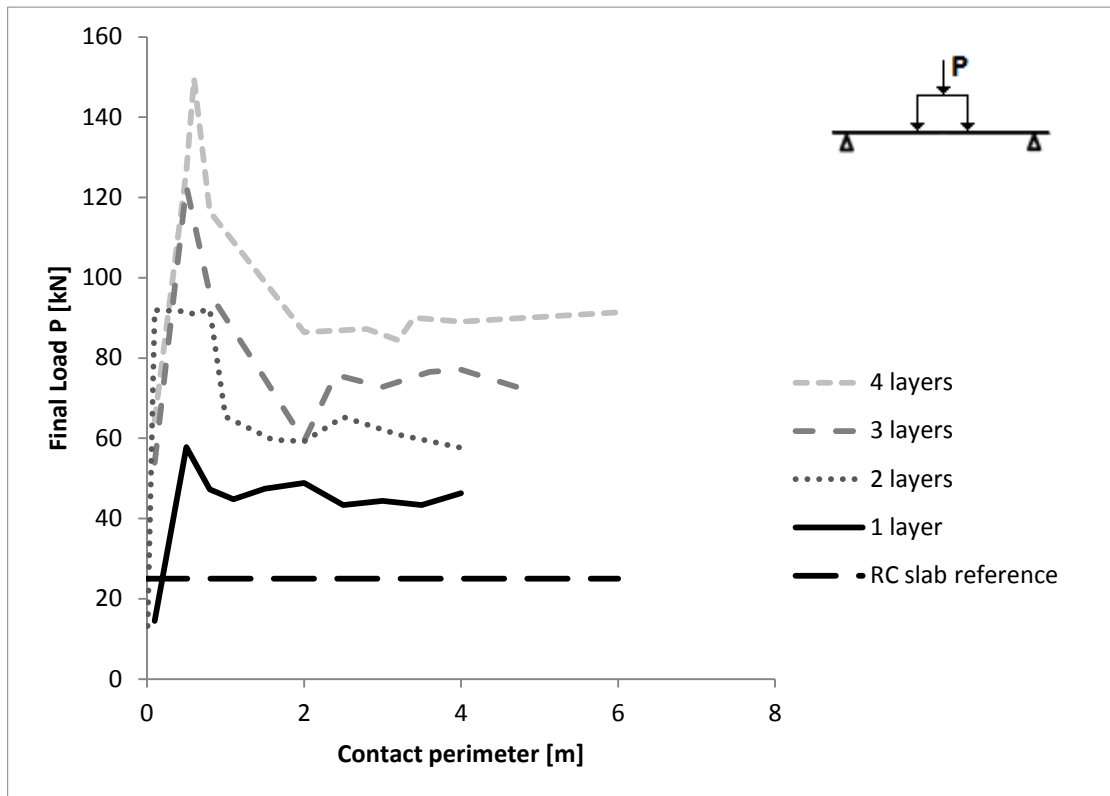
Figure 30   Influence of the contact perimeter on the final load.

Furthermore, the model with 1 layer of textile mesh is analysed, with focus on the influence of the contact perimeter. The parametric study indicated that the optimal value for the perimeter was around 0.5 m. In order to understand why the analysis ended for perimeter values inferior or superior to the optimal value, two models were investigated: one with a perimeter of 0.1 m and the other one with a perimeter of 100 m. The load versus deflection curve for the analyses using these extreme perimeter values are compared to that obtained for the optimal value in Figure 31.
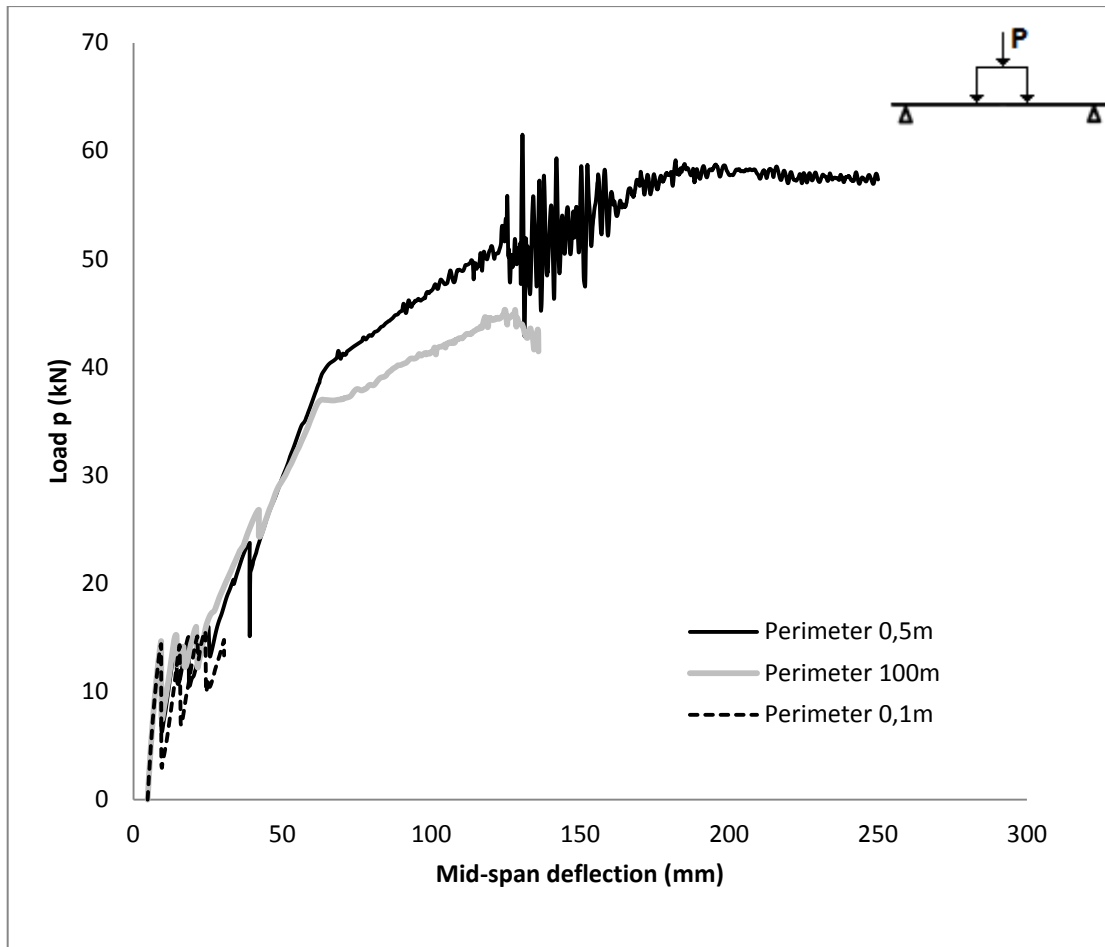
Figure 31   Load- deflection curve, influence of the contact perimeter

It is observed in Figure 31 that for the case of a perimeter of 0.1 m, the bond interaction between textile and concrete became weak; thus, led to an early failure of the slab. As for a perimeter of 100 m, the interaction between reinforcement and concrete was overestimated (i.e. too strong), therefore crushing of concrete appeared in the compression zone. These observations explained why the large variations of the perimeter cause the analysis to stop earlier than expected. As for the models of 2, 3 and 4 layers, the same investigation was executed and a similar behaviour was observed

5.2.4 Analysis of failure modes

In this part different failure modes are discussed in the case of the model with full interaction bond and the models with interface elements and various contact perimeter values. Table 7 below illustrates the influence of these parameters on the failure mode of the FE models.

Table 7   Summary of failure modes in FE models with different Contact Perimeters (CP) and full interaction bond.

cases	parameter	final deflection [mm]	final load [kN]	$\sigma_{textile}$ [MPa]	$\sigma_{concrete}$ [MPa]	σ_{bond} [MPa]	textile slip [mm]	failure mode
1 layer	Bond slip CP=0.1 m	30	15.6	369	17.8	1.6	0.3	weak bond
	Bond slip CP=0.5 m	180	57.8	1200	38	1.7	1.06	textile failure and crushing of concrete in compression zone
	Bond slip CP=100 m	136	45.0	741	40.3	0.03	≈ 0	crushing of concrete in compression
	Full interaction bond	158	57.1	1200	43.3	-	0	textile failure and crushing of concrete in compression zone
2 layer	Bond slip CP=0.01 m	22	15.3	173	15.4	1.5	0.25	weak bond
	Bond slip CP=0.5 m	222	91.4	1200	39.5	1.7	1.18	textile failure and crushing of concrete in compression zone
	Bond slip CP=100 m	102	53.4	497	37.8	0.04	≈ 0	crushing of concrete in compression
	Full interaction bond	211	89.2	1200	40.8	-	0	textile failure and crushing of concrete in compression zone
3 layer	Bond slip CP=0.1 m	74	55.8	357	28.6	1.6	0.5	weak bond
	Bond slip CP=0.5 m	236	122.8	1169	38.8	1.8	1.4	crushing of concrete in compression
	Bond slip CP=100 m	127	75.6	577	39	≈ 0	≈ 0	crushing of concrete in compression
	Full interaction bond	211	112.9	1122	39.8	-	0	crushing of concrete in compression
4 layer	Bond slip CP=0.1 m	78	65.1	356	29.1	1.8	0.5	weak bond
	Bond slip CP=0.6 m	243	149.6	1129	39.9	2	0.8	crushing of concrete in compression
	Bond slip CP=100 m	119	87.2	460	41.6	≈ 0	≈ 0	crushing of concrete in compression
	Full interaction bond	180	121.5	896	40.1	-	0	crushing of concrete in compression

The behaviour of the FE models showed in Table 7 can be divided into three categories regarding the values of the contact perimeter:

- Small values of the contact perimeter: the perimeter was underestimated such that the bond between textile and concrete was too weak. Hence, the tensile efforts cannot be entirely transferred to the textile mesh. It was assumed that for this reason the analysis could not go further; the concrete could not reach its compressive strength and the textile layer did not achieve its yielding point. The exact failure mode remained uncertain.
- Optimum values of the contact perimeter: the 'peak' value of the perimeter was used and the bond was effective. Hence, the textile and steel reinforcement reached their yielding point. Also, the concrete was beyond its compressive strength. Therefore, it can be concluded that the failure of the slab was caused by the failure of textile and the crushing of concrete in the compression zone.
- Enormous values of the contact perimeter: the bond strength was over-estimated and the slip between textile and concrete was close to zero. Yielding was not reached neither in textile nor steel reinforcement. Crushing of concrete appeared in the compression zone which caused the failure of the slab.

The model with full interaction bond shows the following particularities regarding the failure mode:

- In all four cases of strengthening the crushing of concrete occurs in the compression zone. This failure mode was expected, due to the fact that the slip is not allowed.
- The transfer of tensile stresses from concrete to textile is adequate in the cases of 1 and 2 layers of TRC, where the carbon yarns reached their yielding point. Therefore, the cause of failure was observed to be the fracture of textile and the crushing of concrete in the compression zone.
- For the models with 3 and 4 layers of TRC crushing of concrete appeared in the compression zone which caused the failure of the slab. The analysis stopped before the yielding of textile reinforcement. The reasons of that behaviour remained uncertain.

6 Conclusions and outlook

6.1 Conclusions

The aim of this Master's Thesis was to model and analyse the effects of strengthening RC structures using TRC layers. The study particularly focused on the modelling of a TRC strengthened RC slab in DIANA FX+ software. The results showed that the RC slabs strengthened with TRC present significant increase in the load-bearing capacity compared to the unstrengthened RC slabs. Furthermore, for a similar load level, the deflection was reduced in the case of strengthened slabs. The hand calculations of the ultimate load and final deflection were consistent with the numerical results.

A secondary objective was to validate the developed model by means of experimental and numerical results from literature. The simulation results obtained from the developed FE models were consistent with experimental values from Schladitz (2012), in terms of final load and deflection.

An investigation of the sensitivity of critical modelling parameters namely, bond-slip behaviour and textile reinforcement contact perimeter, was included in this study. Bond-slip behaviour between concrete and reinforcement using interface elements was found to be beneficial in regards to achieving more realistic results. The contact perimeter between the textile reinforcement and the concrete body proved to have an important influence in the development of the FE models. Furthermore, this parameter's behaviour presented a peak value for which the interaction between textile and concrete was optimal. In this case, the failure of the slab was caused by textile fracture and crushing of concrete in the compression zone. For small values of the contact perimeter the bond was too weak which caused the analysis to stop prematurely. For extreme values of the contact perimeter, crushing of concrete in the compression zone caused the failure and thus perfect bond behaviour (i.e. embedded reinforcement) was observed.

This project has shown that strengthening RC slabs with TRC layers is an efficient rehabilitation method. Lastly, it is anticipated that this new concept will be further developed and become widely used for the rehabilitation of concrete structures.

6.2 Suggestions for further research

This study can be further developed by deeper investigations such as:

- Modelling the strengthening textile layers separately with fine-grained concrete included, in order to obtain an improved observation of the bonding behaviour between new / old concrete and new concrete / textile reinforcement.
- Micro-scale modelling highlighting the influence of transversal yarns in order to take into account the complex geometry of the textile mesh.
- 3D modelling of slabs with two-directional behaviour of the bond between textile mesh and concrete.
- More detailed parametric study of the contact perimeter between textile reinforcement and concrete.
- Optimising the length of TRC layers and analysis of bond-failure and anchorage length.

7 References

Bosc, J.-L., (2001): Joseph Monier et la naissance du ciment armé, éd. du Linteau, Paris

Brameshuber, W., (2006): Textile Reinforced Concrete - State-of-the-Art Report of RILEM TC 201-TRC

Bruckner, A., Ortlepp, R., Curbach M., (2006): Textile reinforced concrete for strengthening in bending and shear

Bruckner, A., Ortlepp, R., Curbach M., (2008): Anchoring of shear strengthening for T-beams made of textile reinforced concrete (TRC)

CEB (2010) CEB-FIP Model Code 2010. Bulletin 55, Lausanne Switzerland

Davis, B., (2007): Natural fibre reinforced concrete http://people.ce.gatech.edu/~kk92/natfiber.pdf (website consulted in June 2012)

DIANA (2010): DIANA Finite Element Analysis, User's Manual, release 9.4.3. TNO Building and Construction Research, Delft, Netherlands

DIN 1045-1: Concrete, reinforced and prestressed concrete structures

Groz-Beckert (2010): The Albstadt-Lautlingen bridge: https://news.groz-beckert.com/pages/en_n3_textile_reinforced_concrete_bridge.php5 (website consulted in May 2012)

Hegger, J., Will, N., (2004): Tragverhalten von Textilbewehrtem Beton (Load-Bearing behaviour of TRC) Beton- und Stahlbetonbau 99, Vol. 6, p. 452-455.

Häussler-Combe, U., Hartig, J., (2007): Bond and failure mechanisms of textile reinforced concrete (TRC) under uniaxial tensile loading

Keil, A., Cuypers, H., Raupach, M., Wastiels, J., (2008): Study of the bond in textile reinforced concrete: influence of matrix and interface modification

MatWeb (2012): Properties of SIGRAFIL C30 T050 EPY carbon fibre: http://www.matweb.com (website consulted in April 2012)

Ortlepp, R., Hampel, U., Curbach, M., (2006): A new approach for evaluating bond capacity of TRC strengthening

Schladitz, F., Frenzel, M., Ehlig, D., Curbach, M., (2012): Bending load capacity of reinforced concrete slabs strengthened with textile reinforced concrete

Zandi Hanjari, K., (2008): Load-Carrying Capacity of Damaged Concrete Structures. Licentiate Thesis No. 2008:06, Department of Civil and Environmental Engineering, Chalmers University of Technology, Göteborg, Sweden, 98 pp.

APPENDIX A

HAND CALCULATIONS

Deflection calculations

The initial deflection of the slab was calculated in order to analyse the behaviour of the slab in the uncracked and elastic state.

Due to its geometry, the slab is only one directional in bending, which means that its behaviour can be predicted with a beam approach.

For uniform distributed loads, the deflection is calculated with the following equation, Equation 1, and also according to Figure 32:

$$u = \frac{5}{384} \frac{ql^4}{EI} \tag{1}$$
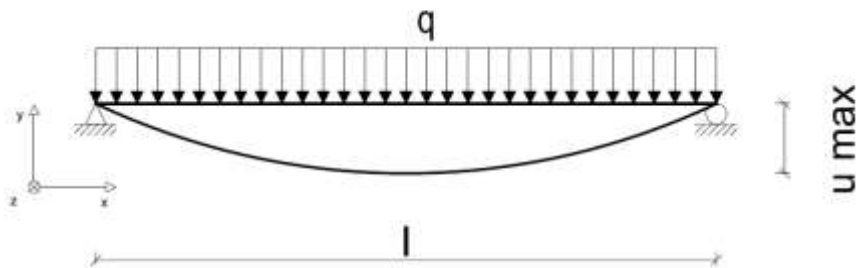
Figure 32   Deflection under uniform distributed load.

Where u is the deflection (in m)

q is the uniform distributed load (in N/m)

l is the span of the slab (in m)

E is the Young's modulus for concrete, here 26 150 MPa

I is the momentum of inertia of the slab in its mid-span (in m^4)

In this case, the uniform distributed load is the self-weight of the entire structure as described below in Equation 2.

$$q = q_{concrete} + q_{TRC} \tag{2}$$

Finally, $q = 6.125 \text{ kN/m}$

The span of the slab, l, is calculated as the distance between the supports to be 6.75 m.

The momentum of inertia of the slab in the mid-span is calculated as the sum of three momentums according to Equation 3:

$$I = I_{concrete} + I_{steel} + I_{textile} \qquad (3)$$

With $\quad I_{concrete} = 122\,551 * 10^{-6} \text{ m}^4$

$\qquad I_{steel} = 3.39 * 10^{-6} \text{ m}^4$

$\qquad I_{textile} = 2.15 * 10^{-6} \text{ m}^4$

It is clear that the reinforcement's influence on the initial deflection of the slab is very small. After the cracking of the concrete occurs, the textile as well as the steel bars will play a more important role in the stiffness of the slab.

The deflection caused by the self-weight, $u_{self\text{-}weight}$, can be calculated to be 5.14 mm.

The deflection caused by the point force P can be calculated with the following equation, Equation 4, along with Figure 33.

$$u(x) = \frac{\frac{P}{2}bx}{6lEI}(l^2 - x^2 - b^2) \qquad (4)$$
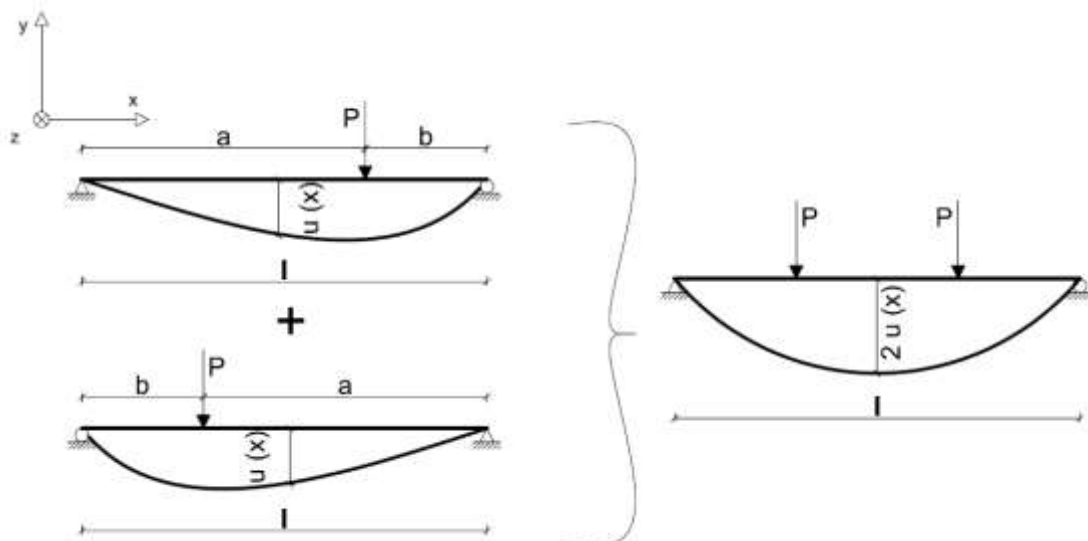
Figure 33   Deflection under point load

Where

u   is the deflection (in m)

P   is the point load (in N)

b   is the distance from the application point of the load and the support, according to Figure 29.

x   is the distance from the support where the deflection is calculated, according to Figure 29.

l   is the span of the slab (in m)

With the same variables as in the previous calculus, the deflection in the mid-span is calculated in function of the variable P, the point load.

The load P versus total deflection is plotted below in Figure 34.
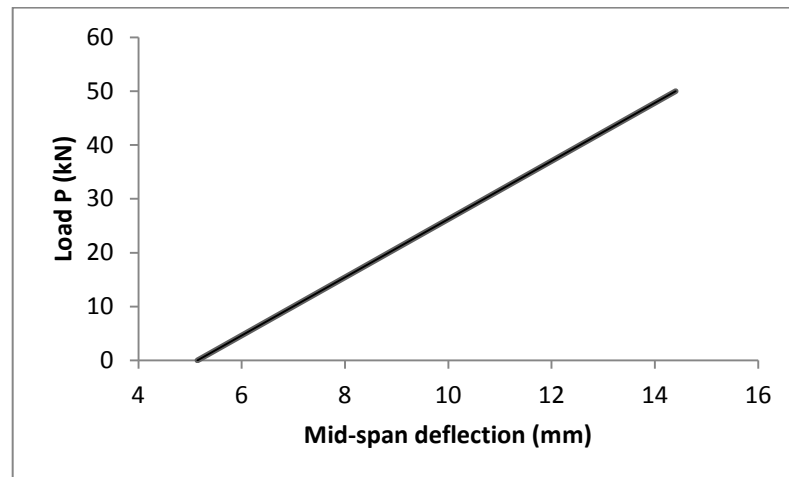
Figure 34   Load-deflection by hand calculations.

The calculated stiffness of the slab is

$$K_{slab} = 5.4 * 10^6 \text{ N/m}$$

This value is compared with the initial stiffness of the FE model in Chapter 5.

Ultimate moment calculations

In this part the ultimate moments were calculated, following the method presented in Schladitz (2012).

The first simplifications considered that the Navier-Bernoulli's hypothesis is accepted, meaning that the cross-sections remain planes and orthogonal to fibres after deformation. Furthermore, a rectangular stress distribution within the concrete compression zone was considered, see Figure 35 .
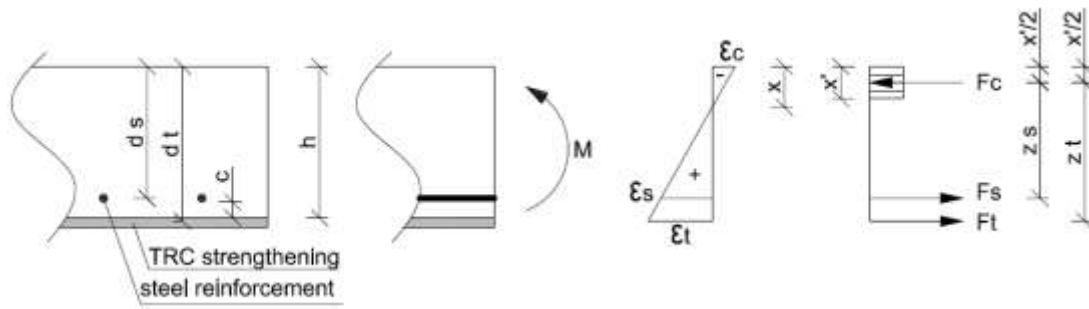
Figure 35 Slab cross-section, strains and forces (based on Schladitz et al ,2012).

The relation between strains can be defined by Equation 5:

$$d_s \frac{\varepsilon_c + \varepsilon_s}{\varepsilon_s} = d_t \frac{\varepsilon_c + \varepsilon_t}{\varepsilon_t} \tag{5}$$

Assuming that the steel reinforcement yielded in the ultimate state of the bearing load capacity (for steel f_y=574 MPa, E=210 000 MPa), the steel strain is calculated according to Equation 6:

$$\varepsilon_s = \frac{f_y}{E} = 2.73 \text{ \textperthousand} \tag{6}$$

and in the yielded state it is $\varepsilon_s > 2.73$ ‰.

According to Figure 32, the distance d_s is calculated, using Equation 7:

$$d_s = h - c - \frac{\varnothing_s}{2} = 0.194 \; m \tag{7}$$

Where h=0.245 m   the thickness of the slab

c=0.03 m   the concrete cover

$\varnothing_s = 0{,}012$ =0.012 m diameter of the steel bar in the mid-span

Therefore $d_s = 0.194$ m

For the textile layers

$d_t = 0.235$ m

Assuming that the concrete has reached its maximum compression strain,

$\varepsilon_c = 3.5$ ‰

And the textile has reached its maximum tensile strength

$\varepsilon_t = 12$ ‰

The height of the compression zone in concrete is calculated according to Equation 8:

$$x = d_t \frac{\varepsilon_c}{\varepsilon_c + \varepsilon_t} \tag{8}$$

Assuming a rectangular distribution of the stress, the value of this height is corrected according to Equation (9):

$$x' = 0.8x \tag{9}$$

The internal lever arms for steel and textile reinforcement are calculated using Equation 10 and Equation 11, respectively:

$$z_s = d_s - \frac{x'}{2} \tag{10}$$

$$z_t = d_t - \frac{x'}{2} \tag{11}$$

These values are calculated for every case (i.e.1,2,3 and 4 layers of textile):

Table 8   Summary of variables in each strengthening case.

Values	1 layer	2 layers	3 layers	4 layers
x (m)	0.053	0.053	0.053	0.054
x' (m)	0.042	0.042	0.043	0.043
zs (m)	0.173	0.173	0.173	0.173
zt (m)	0.212	0.213	0.215	0.216

The tensile forces in the steel and textile reinforcements were calculated according to Equation 12 and Equation 13, respectively:

$$F_s = f_y A_s \tag{12}$$

$$F_t = f_t A_t \tag{13}$$

Where

A_s the cross-section of the steel reinforcement, $A_s=5.65$ cm^2

A_t the cross-section of the textile reinforcement $A_t=n*1.76$ cm^2, n – number of layers

The failure moment Mu of the slab is calculated according to Equation (14):

$$M_u = M_s + M_t = F_s z_s + F_t z_t \qquad (14)$$

Table 9   *Summary of results.*

Values	1 layer	2 layers	3 layers	4 layers
F_s (kN)	324.59	324.59	324.59	324.59
F_t (kN)	211.20	422.40	633.60	844.80
M_u (kNm)	100.90	146.20	192.08	238.53

Verification of the compressive stress in the concrete, σ_c is done below. The concrete force is calculated according to Equation (15):

$$F_c = F_s + F_t = A_s f_y + A_t f_t \qquad (15)$$

Where

   $A_c = b_{slab} x'$ is the area of concrete in compression

   b_{slab} is the width of the slab

Table 10   *Results for the area of concrete in compression*

Case	b_{slab} (m)	x' (m)	A_c (m^2)
1 layer	1	0.042	0.042
2 layers	1	0.042	0.042
3 layers	1	0.043	0.043
4 layers	1	0.043	0.043

To avoid the crushing of concrete in the compression zone the following relation must be respected:

$$\sigma_c = \frac{F_c}{A_c} < \chi f_{cm} \qquad (16)$$

χ=0.95   attenuation coefficient, according to German Standards, DIN 1045-1

The calculated compressive stress in concrete was inferior to the compressive strength of the concrete, see *Table 11*.

Table 11   *Results of compressive stress in concrete.*

Case	F_c (kN)	A_c (m^2)	σ_c (MPa)	f_{cm} (MPa)
1 layer	535.8	0.042	12.8	38
2 layers	747.0	0.042	17.8	38
3 layers	958.2	0.043	22.3	38
4 layers	1169.4	0.043	27.2	38

These values of the ultimate moments were compared to the experimental and FE model's results in Chapter 5.

APPENDIX B

THORENFELDT'S CURVE

Initially, ideal-plastic behaviour of concrete in compression was used. Afterwards, for better description of concrete compression failure mode, it was necessary to include the softening of concrete in compression and to include the downward trend of the stress-strain curve. For this purpose, the Thorenfeldt curve was used. However, this curve is related with the size of the concrete specimen. The relationship has been defined for 300 mm long cylinders, according to Zandi Hanjari (2008). The concrete element size for FE analysis is 10 mm, so Thorenfeldt softening curve was modified by multiplying value of softening branch by size of cylinder divided by size of FE concrete element. The reason for this modification was an assumption that the compressive failure can take place in one element row. Accordingly, the modified curve is shown in Figure 36.
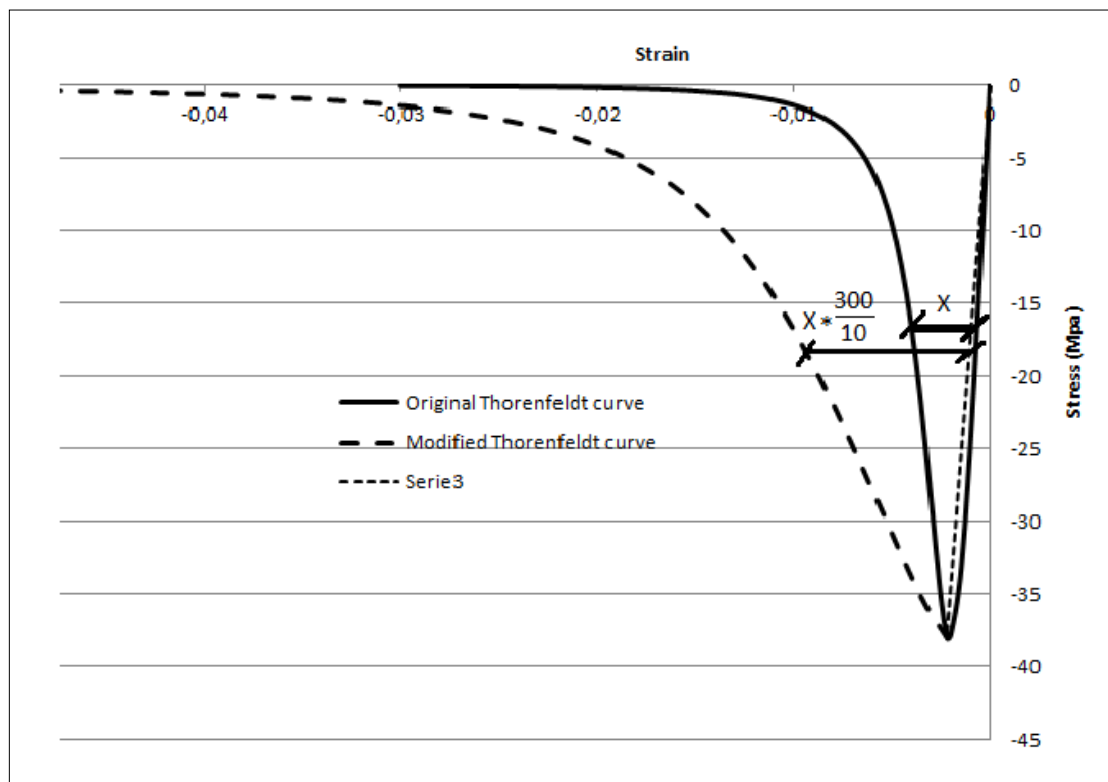
Figure 36   Thorenfeldt modified curve.

This curve is described by Equation 1, as per DIANA (2010):

$$f = f_p \frac{\alpha}{\alpha_p} \left(\frac{n}{n - \left(1 - \left(\frac{\alpha_p}{\alpha_p} \right)^{nk} \right)} \right) \qquad (17)$$

Where

$$f_p = \beta_{\sigma cr} f_{cf}$$

$$\alpha_p = \beta_{\varepsilon cr} \varepsilon_p$$

$$\beta_{\sigma cr} = \beta_{\varepsilon cr} = 1$$

$$f_{cf} = f_{cc} = 38 \, MPa$$

$$n = 0.8 + \frac{f_{cc}}{17} \tag{18}$$

$$k = \begin{cases} 1 \; if \; \alpha_p < \alpha < 0 \\ 0.67 + \dfrac{f_{cc}}{62} \; if \; \alpha \leq \alpha_p \end{cases}$$

APPENDIX C

DATA FILE FOR FE MODEL, FIRST PHASE – SELF WEIGHT

Translated from FX+ for DIANA neutral file (version 1.2.0).

```
'UNITS'
FORCE N
LENGTH M

'DIRECTIONS'
   1  1.00000E+000   0.00000E+000   0.00000E+000
   2  0.00000E+000   1.00000E+000   0.00000E+000
   3  0.00000E+000   0.00000E+000   1.00000E+000
   4  0.00000E+000  -1.00000E+000   0.00000E+000

'COORDINATES'
   1  3.00000E-002   2.15000E-001   0.00000E+000
   2  3.00000E-002   2.15000E-001   0.00000E+000
   3  4.00000E-002   2.15000E-001   0.00000E+000
   4  5.00000E-002   2.15000E-001   0.00000E+000
              .
              .
              .
```

Input for material properties

```
'MATERI'
   1 NAME    "concrete"      ------ The concrete body

     YOUNG   2.61500E+010 ------ Young's modulus
     POISON  2.00000E-001 ------ Poison's ratio
     DENSIT  2.40000E+003 ------ Density
     TOTCRK ROTATE         ------ Rotating total strain model
     TENCRV HORDYK         ------ Tensile curve
     TENSTR  2.90000E+006 ------ Tensile strength
     GF1     140.5         ------ Fracture energy
     CRACKB  1.00000E-002 ------ Crack band width
     COMCRV MULTLN         ------ Compressive curve
     COMPAR 0 0
             -6.53E+6  -0.00025
             -7.84E+6  -0.0003
             -10.43E+6 -0.0004        Multilinear definition of
             -11.72E+6 -0.00045       the compressive curve
             .
             .
             .


     COMSTR  3.8000E+007  ------ Compressive strength
```

```
    2 NAME    "steel_reinf"  ------  The steel reinforcement
      YOUNG   2.10000E+011
      POISON  3.00000E-001
      DENSIT  7.80000E+003
      YIELD   VMISES            ------  Yielding criterion
      YLDVAL  5.74000E+008  ------  Yielding value

    3 NAME    "carbon_yarn"  ------  The textile reinforcement
      YOUNG   1.0000E+011
      POISON  2.00000E-001
      DENSIT  1.80000E+003
      YIELD   VMISES            ------  Yielding criterion
      YLDVAL  1.20000E+009  ------  Yielding value


    4 NAME    "textile_int"  ------  The textile interface material
      DSTIF   1E+10   7.44E+10  ---  Normal and shear stiffness
      BONDSL  3                 ------  Multilinear bond-slip curve
      SLPVAL  0 0
3.35000E+006  4.50000E-005
2.00000E+006  1.30000E-004
1.25000E+006  2.25000E-004         ─  Values for bond-slip curve
            .
            .
            .


    5 NAME    "steel_int"    ------  The steel interface material

      DSTIF   1.00000E+012  2.98400E+010
      BONDSL  3
      SLPVAL  0 0
9.25000E+006  3.10000E-004
1.23300E+007  6.00000E-004
2.00000E+006  1.00000E-003
2.00000E+006  1.50000E-003
2.00000E+006  2.0000E-003

    6 NAME    "super_stiff"  -----  The stiff 'dummy' beam
      YOUNG   2.00000E+014
      POISON  3.00000E-001
      DENSIT  7800
```

Geometry and Data properties' input

```
'GEOMET'
    1 NAME    "steel_int_3"
      THICK   0.188
      CONFIG  BONDSL
    2 NAME    "steel_int_5"
      THICK   0.314
      CONFIG  BONDSL
    3 NAME    "steel_int_1"
      THICK   0.125
      CONFIG  BONDSL
```

```
    4 NAME    "textile_int"
      THICK   0.8
      CONFIG BONDSL
    5 NAME    "reinf_3"
      CROSSE  2.51000E-004
    6 NAME    "reinf_5"
      CROSSE  8.17000E-004
    7 NAME    "reinf_1"
      CROSSE  5.65000E-004
    8 NAME    "textile"
      CROSSE  0.000176
    9 NAME    "dummy_beam_up"
      RECTAN  1.00000E-001  1.00000E-001
      ECCENT  0   0   0   0
      ZAXIS   0.00000E+000  0.00000E+000  1.00000E+000
   10 NAME    "dummy_beam_do"
      RECTAN  1.00000E-001  1.00000E-001
      ECCENT  0  0   0   0
      ZAXIS   0.00000E+000  0.00000E+000  1.00000E+000
   11 NAME    "concrete"
      THICK   1.00000E+000
'DATA'
   10 NAME    "dummy_beam_up"
   11 NAME    "dummy_beam_do"
    1 NAME    "concrete"
    2 NAME    "reinf_1"
    3 NAME    "reinf_3"
    4 NAME    "reinf_5"
    5 NAME    "textile"
    6 NAME    "steel_int_1"
    7 NAME    "steel_int_3"
    8 NAME    "steel_int_5"

'ELEMENTS'

CONNECT
    1 L8IF    402 1 3 2
    2 L8IF    401 402 4 3
    3 L8IF    400 401 5 4
    4 L8IF    399 400 6 5          Interface elements
      .
      .
      .

  201 L2TRU   1 402
  202 L2TRU   402 401
  203 L2TRU   401 400
  204 L2TRU   400 399             Reinforcement elements (truss)
      .
      .
      .

10845 L6BEN 1570 10354           Stiff beam elements
10846 L6BEN 9641 10355

1095 Q8MEM  1100 1101 1845 1844
1096 Q8MEM  1844 1845 1846 1843
1097 Q8MEM  1843 1846 1847 1842
```

```
1098 Q8MEM  1842 1847 1848 1841      2D concrete elements
       .
       .
       .
```

Assignment of material, data and geometry for 2D elements

```
MATERI
/ 1095-9144 9795-10844 / 1
/ 201-400 601-800 948-1094 / 2
/ 9470-9794 / 3
/ 9145-9469 / 4
/ 1-200 401-600 801-947 / 5
/ 10845 10846 / 6
DATA
/ 10845 / 10
/ 10846 / 11
/ 1095-9469 9795-10844 / 1
/ 948-1094 / 2
/ 201-400 / 3
/ 601-800 / 4
/ 9470-9794 / 5
/ 801-947 / 6
/ 1-200 / 7
/ 401-600 / 8
GEOMET
/ 1-200 / 1
/ 401-600 / 2
/ 801-947 / 3
/ 9145-9469 / 4
/ 201-400 / 5
/ 601-800 / 6
/ 948-1094 / 7
/ 9470-9794 / 8
/ 10845 / 9
/ 10846 / 10
/ 1095-9144 9795-10844 / 11
```

Definition of loads

```
'LOADS'
CASE 1
WEIGHT              self-weight
  2 -9.81

:CASE 2
:DEFORM                           deformation control
:1570 TR 2 -1.E-002
```
                                                    Phased analysis

Element groups

```
'GROUPS'
ELEMEN
   6 "Auto-Mesh(Face)" / 1-200 /
   7 "Auto-Mesh(Edge)" / 201-400 /
  12 "Auto-Mesh(Face)-1" / 401-600 /
```

```
    13 "Auto-Mesh(Edge)-2" / 601-800 /
    18 "Auto-Mesh(Face)-3" / 801-947 /
    19 "Auto-Mesh(Edge)-4" / 948-1094 /
    20 "Auto-Mesh(Face)-5" / 1095-9144 /
    25 "Auto-Mesh(Face)-6" / 9145-9469 /
    26 "Auto-Mesh(Edge)-7" / 9470-9794 /
    31 "Auto-Mesh(Face)-9" / 9795-10844 /
    32 "Auto-Mesh(Edge)-10" 10845
    33 "Auto-Mesh(Edge)-11" 10846
```

Boundary conditions and constraints

```
'SUPPOR'
/ 1473 9302 9979 9980 9301 953 1474-1495 952 / TR 1 ⎤
/ 1473 9302 9979 9980 9301 953 1474-1495 952 / TR 3 ⎬  supports
/ 9641 / TR 2                                        │
:1570 TR 2                                           ⎦
```

```
'TYINGS'
EQUAL TR 1                              ⎤
/ 604 / 805                             │
EQUAL TR 2                              │
/ 604 / 805                             ⎬  Tyings of nodes
ECCENT TR 2                             │
/ 1562-1569 1571-1578 / 1570           │
/ 9637-9640 9642-9645 / 9641           ⎦
```

```
'END'
```

Data file for FE model, second phase – self weight and deformation control

```
PHASE 2

'LOADS'
CASE 1
WEIGHT
  2 -9.81
CASE 2
DEFORM
1570 TR 2 -1.00E-002
'SUPPOR'
/ 1473 9302 9979 9980 9301 953 1474-1495 952 / TR 1
/ 1473 9302 9979 9980 9301 953 1474-1495 952 / TR 3
/ 9641 / TR 2
/ 1570 / TR 2
```

APPENDIX D

COMMAND FILE FOR FE MODEL, FIRST AND SECOND PHASE OF LOADING

```
*FILOS
 INITIA                              First phase
*INPUT
*PHASE


*INPUT
READ TABLE LOADS
READ TABLE SUPPORTS                  Second phase

READ TABLE TYINGS
*PHASE



                                     Common for both phases
BEGIN ACTIVE
 ELEMENT ALL
 REINFO ALL
END ACTIVE
*NONLIN

 BEGIN TYPE
  BEGIN PHYSIC
    END PHYSIC
  END TYPE

 BEGIN OUTPUT
   FXPLUS                            Output saved in file '1' for first phase
   FILE "1"
END OUTPUT

 BEGIN OUTPUT
   FXPLUS                            Output saved in file '2' for second phase
   FILE "2"
END OUTPUT

  BEGIN EXECUTE            —————————  First load; self weight
   BEGIN LOAD
    LOADNR=1
     BEGIN STEPS
      BEGIN EXPLIC
      SIZES 1.0(1)        —————————  First load applied in one step
     END EXPLIC
     END STEPS
    END LOAD
    BEGIN ITERAT
      METHOD NEWTON REGULA  ————————  Iteration method
:     METHOD SECANT BFGS
      MAXITE=100
```

```
:       LINESE
      BEGIN CONVER
        ENERGY CONTIN TOLCON=0.0001  ⎤
        FORCE CONTIN TOLCON=0.01     ⎬─  Convergence criterion
        DISPLA CONTIN TOLCON=0.01    ⎦
      END CONVER
    END ITERAT
    SOLVE GENEL
  END EXECUT

BEGIN EXECUTE        ──────────        Only for second phase
  BEGIN LOAD
    LOADNR=2
     BEGIN STEPS
      BEGIN EXPLIC
      SIZES 0.01(2500)   ──────────    Step size and number of steps
     END EXPLIC
     END STEPS
    END LOAD
    BEGIN ITERAT
      CONTIN
      METHOD NEWTON REGULA   ────────   Iteration method
:      METHOD SECANT BFGS
      MAXITE=350
:       LINESE
      BEGIN CONVER
        ENERGY CONTIN TOLCON=0.0001  ⎤
        FORCE CONTIN TOLCON=0.01     ⎬─  Convergence criterion
        DISPLA CONTIN TOLCON=0.01    ⎦
      END CONVER
    END ITERAT
    SOLVE GENEL
  END EXECUT
*END
```